FINNISH ROAD ADMINISTRATION

Mirva Koskinen, Pauli Vepsäläinen, Matti Lojander

Modelling of Anisotropic Behaviour of Clays

Test Embankment in Murro, Seinäjoki, Finland

Finnra Reports 16/2002

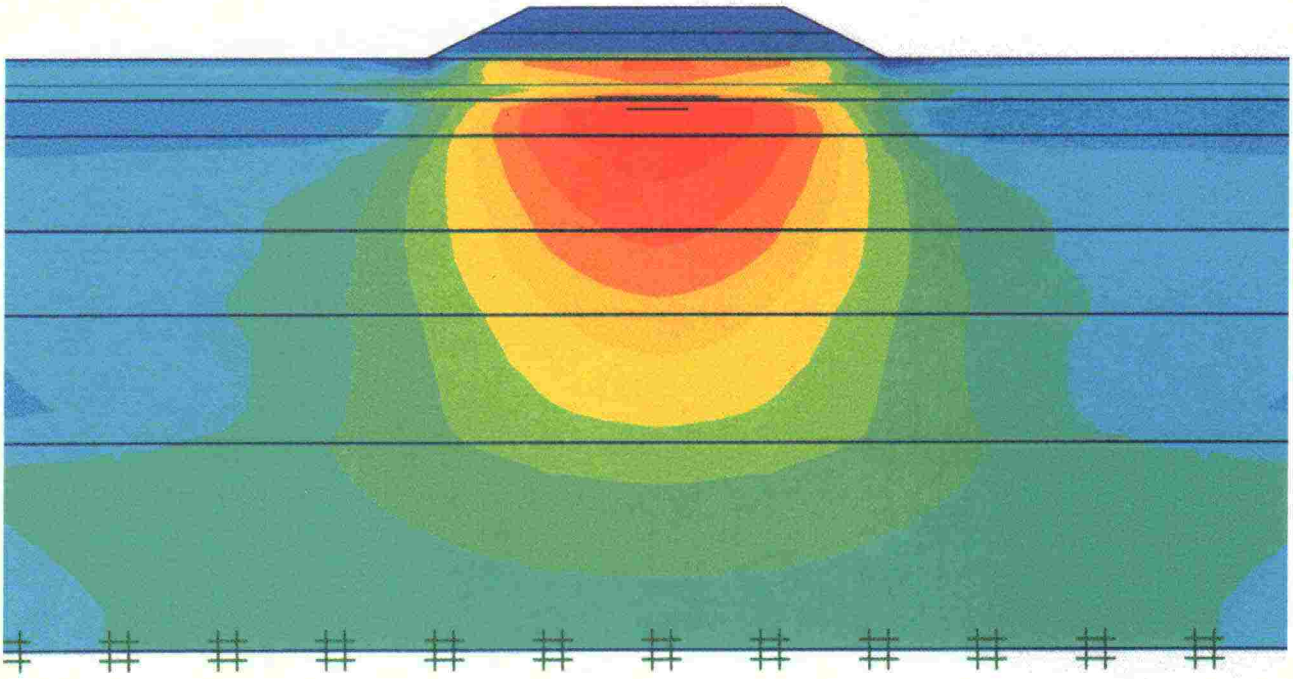

Excess pore pressure immediately after construction

Mirva Koskinen, Pauli Vepsäläinen, Matti Lojander

Modelling of Anisotropic Behaviour of Clays

Test Embankment in Murro, Seinäjoki, Finland

Finnra Reports 16/2002

FINNRA
Helsinki 2002

ISSN 1457-9871
ISBN 951-726-883-1
TIEH 3200748E

Edita Prima Oy
Helsinki 2002

This publication is available at:
Finnra Publications Sales
fax int. +358 204 22 2652
e-mail julkaisumyynti@tiehallinto.fi
www.tiehallinto.fi/julk2.htm

Painotuote

Finnish Road Administration
Opastinsilta 12 A
PB 33
FIN-00521 HELSINKI
Phone int. +358 204 22 11

Mirva KOSKINEN, Pauli VEPSÄLÄINEN, Matti LOJANDER: Modelling of anisotropic behaviour of clays, Test embankment in Murro, Seinäjoki, Finland. Helsinki 2002. Finnish Road Administration. Finnra Reports 16/2002. 63 p. + app. 5 p. ISSN 1457-9871, ISBN 951-726-883-1, TIEH 3200748E.

Keywords: subsoil, clay, embankment, settlement, soil mechanics, model, test
Classification: 62

ABSTRACT

In 1993 Finnish Road Administration started a study considering a test embankment in Murro, Seinäjoki. The object of the project was to use the information in design and renovations of roads built on soft soils. This report is the final report of the project and it is a part of a project the Finnish Road Structures Research Programme, TPPT. This report concerns site investigations and laboratory tests carried out before and after construction. In addition, the behaviour of the embankment was modelled with programs PLAXIS and SAGE CRISP, and the calculated results were compared with the observations. A new soil model, referred here with the name SS-CLAY1, developed at University of Glasgow in collaboration with Helsinki University of Technology based on projects funded by EU and Finnish Academy is also presented. The model takes the structure of the clay, i.e. anisotropy and bonding into account. A triaxial test series on Murro clay carried out for testing the model is presented.

The test embankment was constructed without lateral berms in two layers in March 1993. Before construction site investigations and sampling were made in the embankment area. According to those, the subsoil is normally consolidated sulphide-rich silty clay and clayey silt. The depth of the deposit is 23 meters and 1,6 meters of it is heavily overconsolidated dry crust. The subsoil can be roughly divided into two approximately equally thick layers and the upper one is clearly softer than the lower one.

The embankment was instrumented with pore pressure probes, settlement plates, inclinometers and extensometers. The observed total settlement in eight years was 798 mm and the observed maximum horizontal displacement was 123 mm. Samples taken under the embankment eight years after construction and tested in the laboratory show that the water content and the void ratio have decreased in the upper layer, which is approximately 10 meters thick and where the settlements have occurred.

The settlements calculated with PLAXIS correspond fairly well to the observations. The soil was modelled with the Soft Soil model. The calculations with SAGE CRISP using Modified Cam Clay model give quantitatively same results. The calculated horizontal displacements with both programs are good, except for the predicted depth of the maximum horizontal displacement. The growth of the undrained shear strength calculated with PLAXIS is up to 9 kPa, but the observations do not support this, which is partly due to the unreliability of the field vane test results. SAGE CRISP was able to model the decrease of the void ratio due to consolidation in the settling soil layers as well.

Mirva KOSKINEN, Pauli VEPSÄLÄINEN, Matti LOJANDER: Modelling of anisotropic behaviour of clays, Test embankment in Murro, Seinäjoki, Finland. Helsinki 2002. Tiehallinto, Finnra reports 16/2002. 63 s. + liitt. 5 s. ISSN 1457-9871, ISBN 951-726-883-1, TIEH 3200748E.

Asiasanat: pohjamaa, savi, penkereet, painumat, maamekaniikka, malli
Aiheluokka: 62

TIIVISTELMÄ

Vuonna 1993 Tielaitos käynnisti Seinäjoella sijaitsevaa Murron koepengertä koskevan lujittumistutkimuksen. Tarkoitus oli käyttää saatuja tietoja pehmeiköille perustettujen teiden suunnittelussa ja korjausrakentamisessa. Tämä raportti on projektin loppuraportti, ja se on osa projektia S4 Tien pohjarakenteet. Tässä raportissa on käsitelty koepenkereen alueelta tehtyjen pohjatutkimusten ja laboratoriokokeiden tuloksia sekä ennen että jälkeen rakentamisen. Lisäksi koepenkereen käyttäytymistä on mallinnettu ohjelmilla PLAXIS ja SAGE CRISP ja saatuja tuloksia analysoitu kahdeksan vuoden aikana kerättyjen havaintojen valossa. Esiteltiin Glasgow'n yliopistossa yhteistyössä Teknillisen korkeakoulun kanssa EU:n ja Suomen Akatemian rahoittamien projektien yhteydessä kehitetty malli, jota tässä kutsutaan nimellä SS-CLAY1 ja joka ottaa huomioon saven rakenteen, eli anisotropian ja partikkelien väliset sidokset. Esiteltiin mallin testaamista varten Murron savella tehty kolmiaksiaalikoesarja.

Koepenger rakennettiin ilman vastapenkereitä kahdessa kerroksessa maaliskuussa 1993. Ennen rakentamista penkereen alueella tehtiin kairauksia ja otettiin sekä häiriintyneitä että häiriintymättömiä näytteitä. Näiden perusteella voidaan todeta pohjamaan olevan normaalisti konsolidoitunutta sulfidipitoista laihaa savea ja savista silttiä. Kerrostuman paksuus on 23 metriä, josta noin 1,6 metriä on voimakkaasti ylikonsolidoitunutta kuivakuorta. Pohjamaa jakautuu kahteen likimain yhtä paksuun kerrokseen, joista ylempi on selvästi heikompi.

Penkereeseen asennettiin huokospaineputkia, painumalevyjä, inklinometreja ja ekstensometreja. Kahdeksan vuoden havaittu kokonaispainuma on 798 mm ja suurin sivusiirtymä 123 mm. Kahdeksan vuoden jälkeen penkereen alta otetut näytteet ja laboratoriokokeet osoittavat, että maan vesipitoisuus ja huokosluku ovat selvästi pienentyneet ylimmässä hieman alle kymmenen metrin paksuisessa kerroksessa, samassa, jossa myös painumat ovat tapahtuneet.

PLAXIS-laskelmilla saadut painumatulokset vastaavat melko hyvin mitattuja. Laskentamallina käytettiin Soft Soil –mallia. SAGE CRISP laskentatulokset Modified Cam Clay -mallilla antavat saman suuruisia tuloksia. Molemmilla ohjelmilla saadut sivusiirtymien arvot ovat suuruusluokaltaan oikeita, mutta maksimi jää lähemmäs maanpintaa kuin havaittu. Ohjelmalla PLAXIS laskettu leikkauslujuuden kasvu on suurimmillaan 9 kPa, mutta havainnoista tälle ei saada tukea, mikä johtuu osaltaan siipikairaushavaintojen epäluotettavuudesta. Ohjelmalla SAGE CRISP saatiin mallinnettua myös konsolidaatiosta aiheutuva huokosluvun aleneminen painuvissa kerroksissa.

PREFACE

The test embankment in Murro, Seinäjoki, Finland was built and instrumented in 1993 by the Finnish Road Administration in order to study the behaviour of soft soil, and collect information that would support to design road embankments and to plan the rehabilitation and reconstruction of roads built on soft soils. The Finnish Road Administration collected observations of settlements, horizontal displacements and pore pressures for eight years. Laboratory tests have been made in the Laboratory of Soil Mechanics and Foundation Engineering at Helsinki University of Technology.

This is the final report of the project. Mirva Koskinen wrote Chapters 1-5, and Chapters 6-7 have been written as teamwork by Pauli Vepsäläinen, Mirva Koskinen and Matti Lojander. The authors would like to thank Karim Kinani for the PLAXIS calculations. The members of the advisory group were Pentti Salo (Finnish Road Administration), and Mikko Smura, Panu Tolla and Jyrki Nikkinen from the Finnish Road Enterprise.

Helsinki, May 2002

Finnish Road Administration

Contents

1 INTRODUCTION

In 1993 a test embankment was set up by the Finnish Road Administration in Murro near the town of Seinäjoki in western part of Finland. The hardening and the changes of the properties of the subsoil due to consolidation in particular were meant to be the main focus. The embankment was well instrumented and observations of settlements, horizontal displacements and pore pressures have been collected for eight years. This data is meant to be applied to the planning of other new roads as well as to the renovation and improvement of old roads that have been built on soft soils.

Calculations with conventional tools are carried out: programs PLAXIS and SAGE CRISP are used and the results are compared to the settlement data of eight years. Similar calculations have been carried out for another test embankment in Haarajoki, Finland as well. A report of those calculations is published in parallel with this report. Both projects are a part of a long-term project TPPT Road Structures Research Program.

In 2000, a four-year Research Training Network, Soft Clay Modelling for Engineering Practice (SCMEP), was established. The network is funded by the European Commission, and it aims to develop simple but realistic and effective design methods for soft soils, and to bring them available for geotechnical design. In the framework of SCMEP, a new elasto-plastic soil model for soft, normally or lightly overconsolidated clays was developed at University of Glasgow in collaboration with Helsinki University of Technology. This model, called SS-CLAY1, combines the effects of natural and strain-induced anisotropy and the effect of de-structuration on soil. Its relative simplicity, the reasonable quantity of parameters and the ability to predict the behaviour of soil rather realistically regardless of stress paths separates SS-CLAY1 from other similar soil models.

The development of the model is continuing in Glasgow and Helsinki within the framework of a 3-year project funded by the Finnish Academy that begun in January 2002. The data from the Murro test embankment is used for testing the soil model SS-CLAY1 both in this report and in the future. Murro clay was chosen because it differs from other Finnish clays that have been studied so far, and because of the comprehensive observations, site investigations and laboratory testing programs that have already been performed. The model SS-CLAY1 is in the process of being implemented to program SAGE CRISP at the University of Glasgow.

2 SITE INVESTIGATIONS AND CALCULATIONS BEFORE CONSTRUCTION

2.1 Site investigations

Four types of boring methods were used at the area of the embankment before construction: Swedish weight sound testing, field vane testing, CPTU-testing (cone penetration testing with a pore pressure probe) and static-dynamic penetration testing. The last method, developed in Finland, combines possibilities to use cone penetration test in cohesive soils and dynamic probing in non-cohesive soils. In addition, both disturbed and undisturbed samples were taken and examined in the laboratory. Results of the site investigations before construction were introduced by Selkämaa (1994). A map of the embankment area with the boreholes is presented in Figure 2.1.

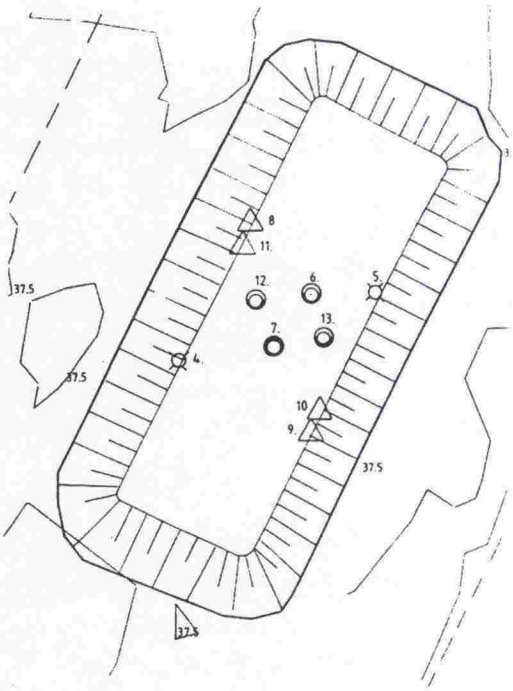

Figure 2.1 Layout of the boreholes. (Selkämaa 1994)

The dry crust was found to be approximately 1,6 meters thick and the depth of the deposit is 23 meters at the maximum. The deposit can be roughly separated into two layers: the upper, softer, layer and the lower, harder, layer. The thickness of these layers is nearly the same. This is indicated in Figure 2.2, which represents Swedish weight sound testing and field vane testing diagrams. The shear strength of the upper layer prior to construction

of the embankment is according to the field vane test 10...20 kPa and of the lower layer 30 kPa. The static-dynamic penetration test and cone penetration test are shown in Figure 2.3.

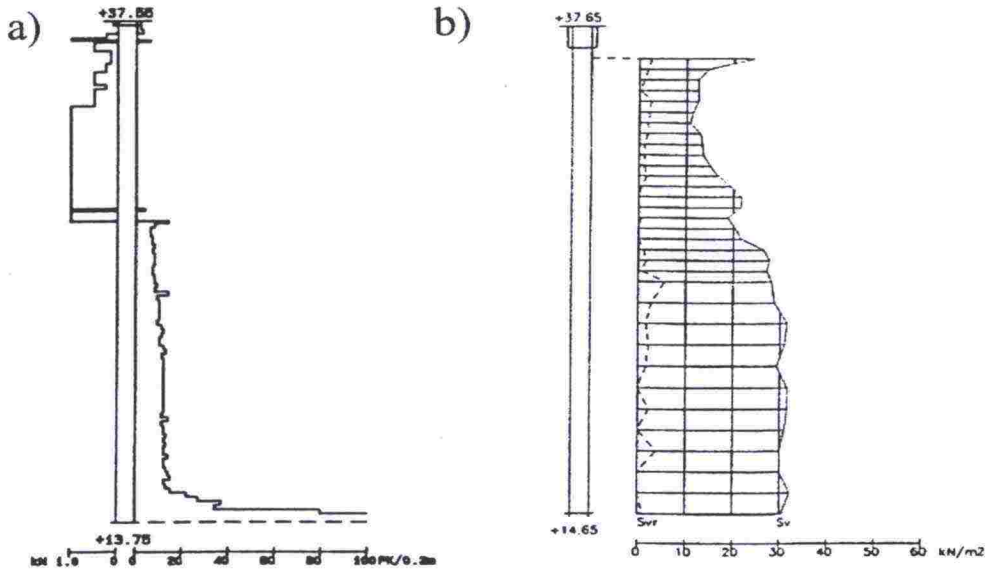

Figure 2.2 *a) Swedish weight sound test, borehole 2. b) Field vane test, borehole 4. (Selkämaa 1994)*

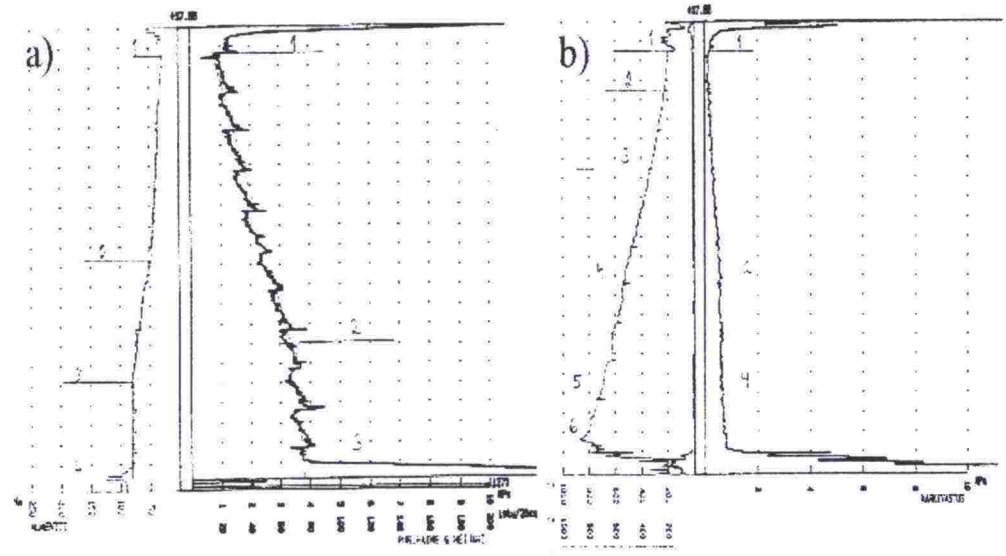

Figure 2.3 *a) Static-dynamic penetration test diagram, borehole 8 and b) CPTU diagram, borehole 10, of Murro clay before the construction of the embankment. (Selkämaa 1994)*

2.2 Laboratory tests

Firstly, the index properties of the samples were defined. The other tests included oedometer tests (standard incremental tests and constant rate of strain tests alike) and triaxial tests. All the tests were carried out in the Laboratory of Soil Mechanics and Foundation Engineering at Helsinki University of Technology. A series of triaxial tests was carried out also at University of Turku. The latter results are not analysed in this report.

Figure 2.4 shows the index properties of Murro clay before the construction of the embankment. The water content of the upper half of the deposit varies between 50 and 100 percent while the water content of the lower half is nearly constant, about 60 percent. The percentage of clay-sized fraction lies just above 30 percent, and therefore the soil is classified as either silty clay or clayey silt. The organic content of the upper part of the deposit is rather high, over 2 percent. The difference between the liquid limit and the water content is very small. However, the soil is not very sensitive.

In Finland, Janbu's (1970) tangent modulus method of Equation (2.1) is commonly used for calculating settlements of both normally consolidated and overconsolidated soils. The parameters, modulus number m and stress exponent β can be determined from oedometer tests.

$$\varepsilon_1 = \frac{1}{m\beta}\left(\frac{\sigma_1}{\sigma_v}\right)^{\beta} + C \qquad (2.1)$$

According to the standard oedometer test results summarized in Figure 2.5, the clay is overconsolidated only on the dry crust, and normally consolidated elsewhere. The values of the modulus number are roughly 5...10 in the upper half and 10...15 in the lower half of the deposit, and the stress exponent lies between 0 and –0.5 in the whole deposit.

The triaxial tests carried out at HUT were consolidation tests and drained or undrained shearing tests. The parameters for Modified Cam Clay were determined from the triaxial tests. The effective cohesion was small, 0...3 kPa, and the effective friction angle varied between 23...37 degrees. The parameters that were used in the calculations in 2001 are based on these triaxial tests, and verified with the results of more recent tests.

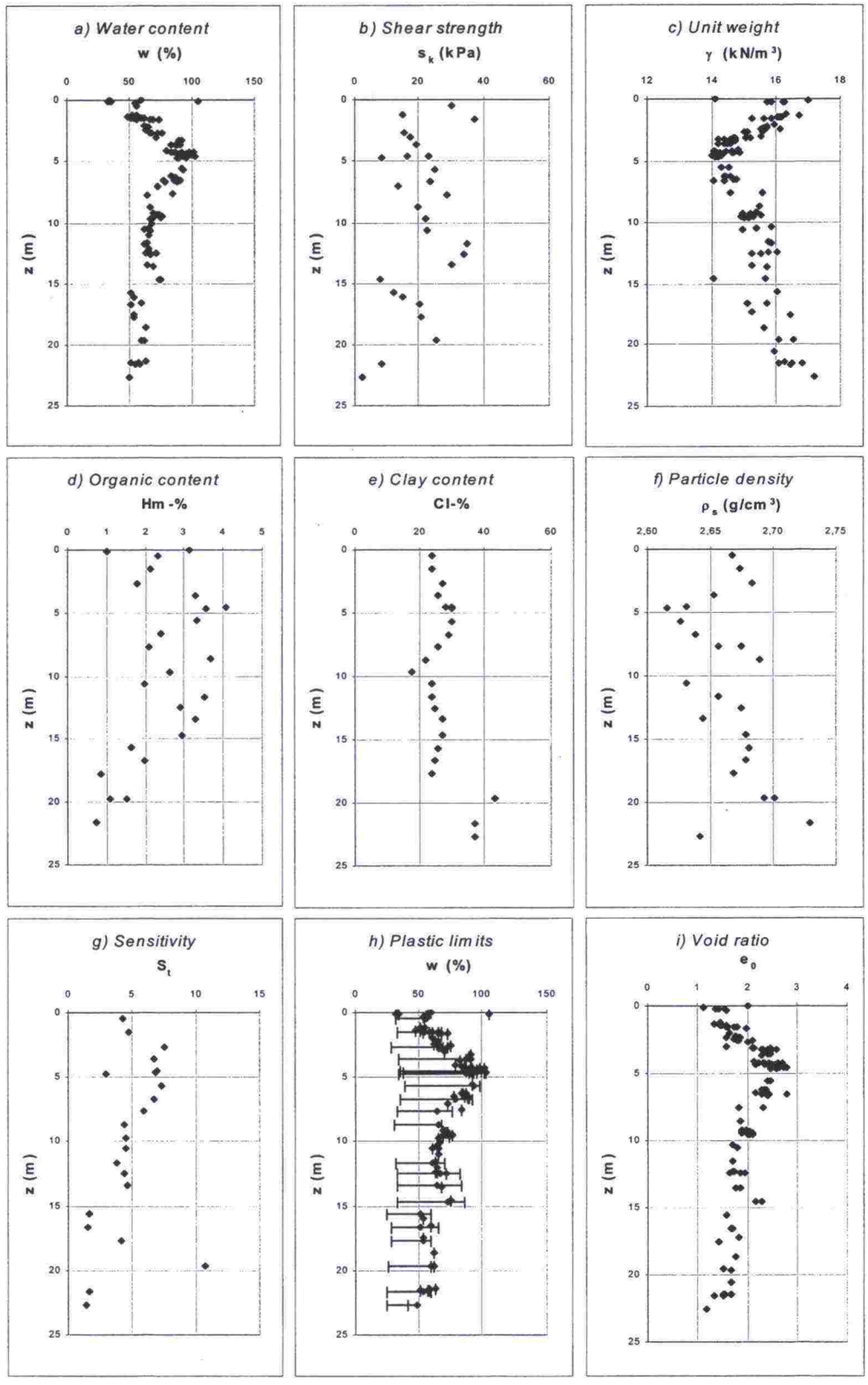

Figure 2.4 *Index properties of Murro clay in 1993, before the construction of the embankment.*

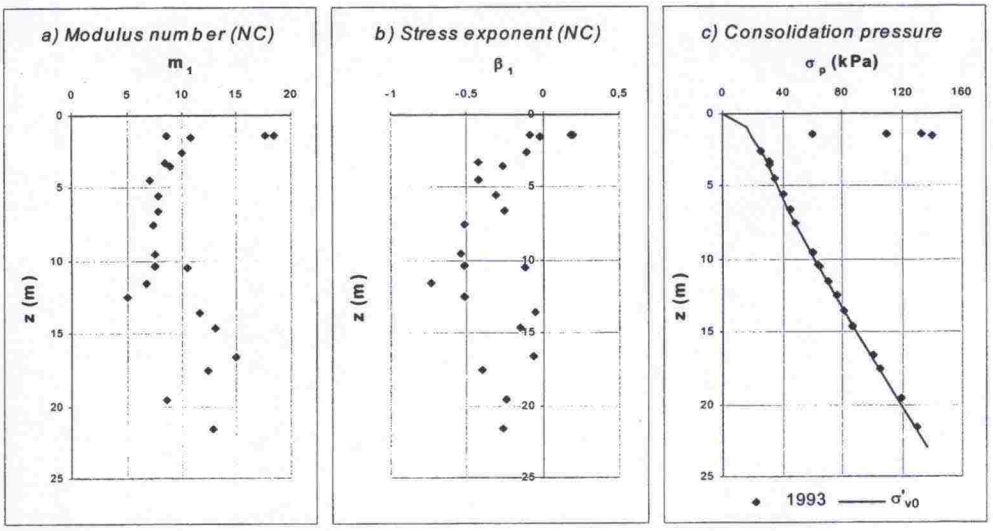

Figure 2.5 *The results of oedometer tests on Murro clay before the construction of the embankment.*

2.3 Calculations

The calculations were performed and presented in detail by Selkämaa (1994). Three things were calculated: stability, the magnitude of settlements and the settlement time. All the calculations were done with program Fulgeo. The calculations are described here shortly and the basic results are presented.

The stability calculations were based on five layers with different shear strengths. The riskiest slip surface goes at a depth of 6,6 meters with a radius of 12 meters. The factor of safety was 1,41.

The number of layers was doubled for calculating the settlements. The settlements were calculated underneath the embankment in three points: in the middle, on the edge and in the half way of the slope of the embankment. The embankment is 2 m high, 10 m wide, and the unit weight of the embankment material is 20 kN/m^3. In the middle of the embankment the calculated settlement was 657 mm and the settlement of the slope was 261 mm. The total settlement time varied between 13.5...235 years depending on the value of the consolidation coefficient c_v. The measured c_v values gave the longest time and when the measured value was multiplied with 15, the shortest time was achieved. The shortest settlement time corresponded to the observed settlements after 10 months. This examination cannot be considered very reliable.

3 OBSERVATIONS

The embankment was constructed between 25th and 26th of March 1993 in two 1-meter thick layers. The material was crushed gravel with grain size of 0...65 mm. The embankment was instrumented with pore pressure probes (u1...u8), settlement plates (L1...L7), extensometers (E) and inclinometers (I1, I2). The layout of the equipment is presented in Figure 3.1. In Figure 3.2, the depths of the pore pressure probes are shown.

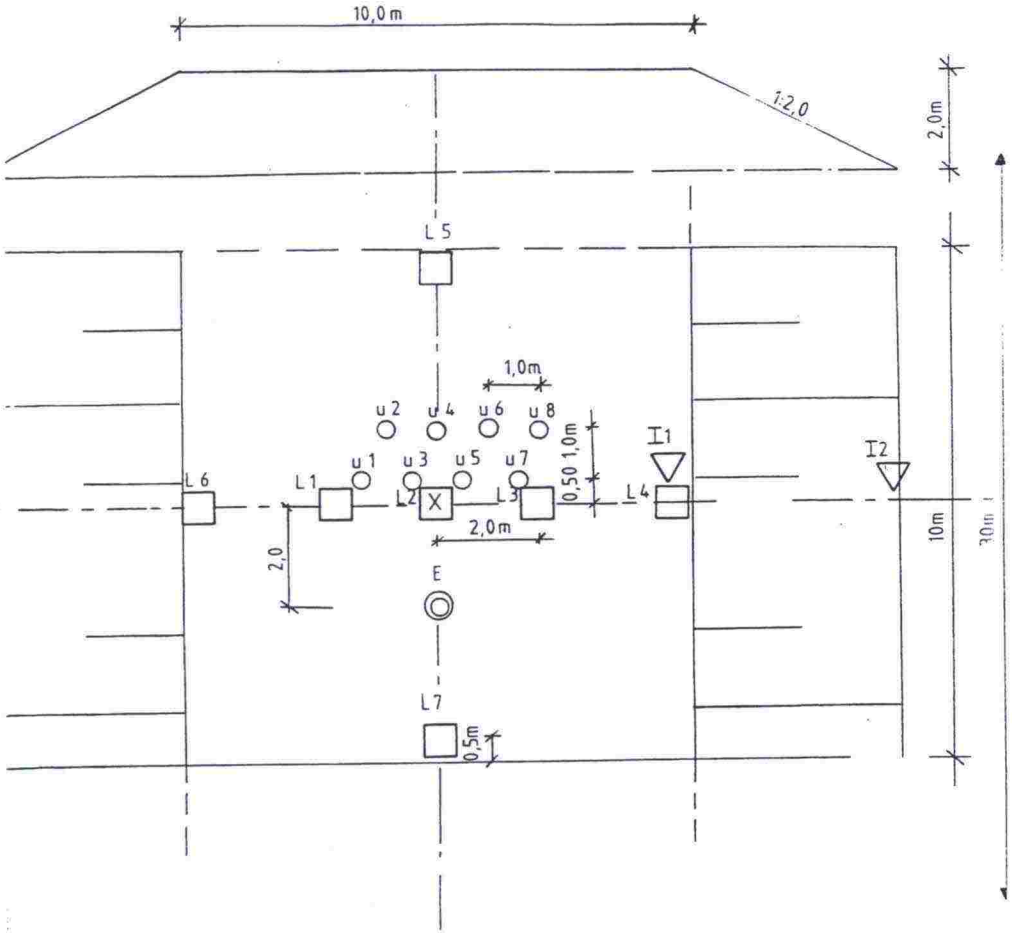

Figure 3.1 Layout of the instrumentation of Murro test embankment. (Selkämaa 1994)

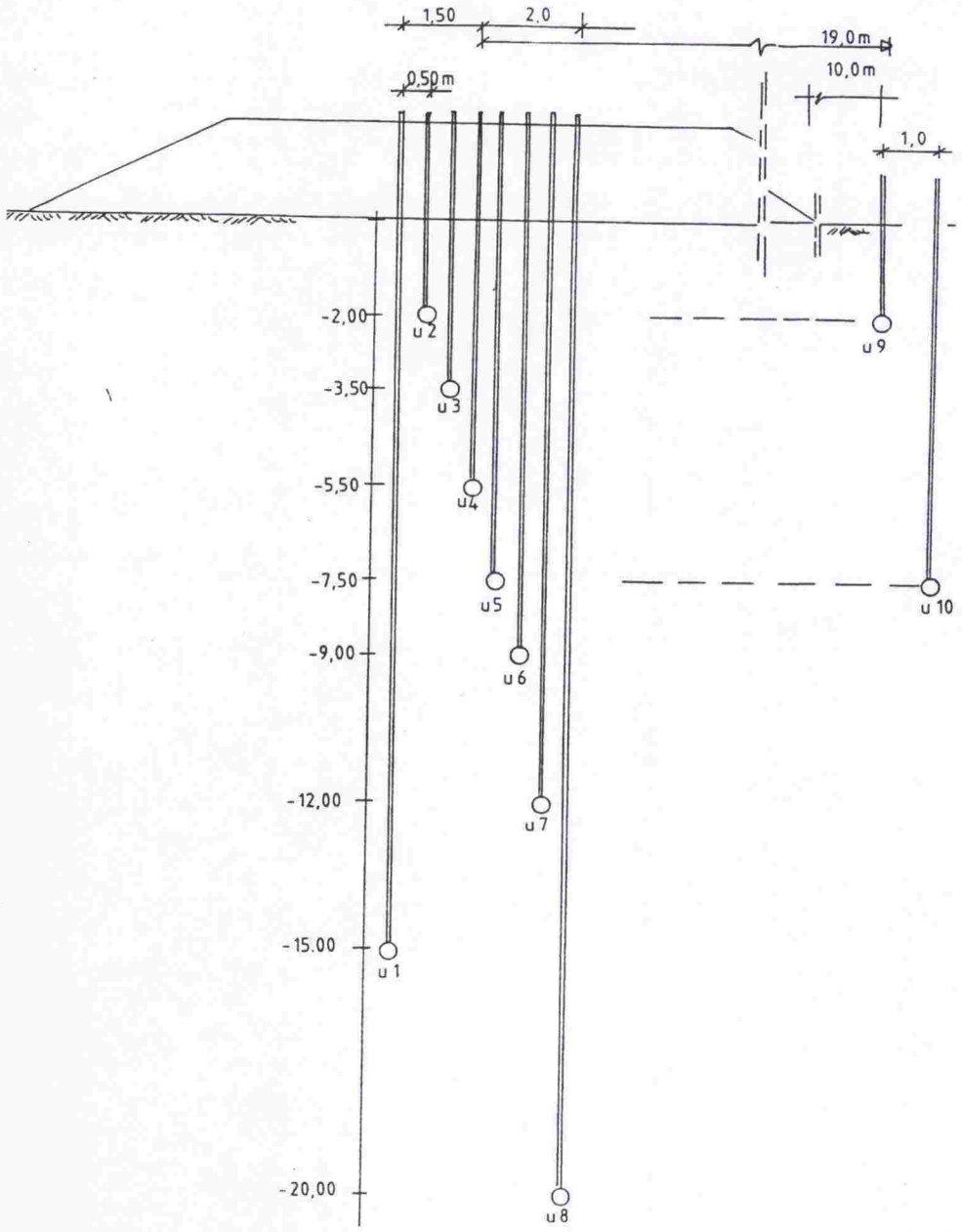

Figure 3.2 Pore pressure probes of Murro test embankment. (Selkämaa 1994)

The observations have been collected for eight years. The evolution of the settlements of the embankment during this period is presented in Figure 3.3. The maximum settlement seems to be located on the centre line of the embankment but not right in the middle, i.e. the plate number L7 that is 10 meters from the centre point has settled more than number L2. The difference is nearly 100 mm. The plate number L5, which is located 10 meters apart from the centre point on the opposite side than L7, seems to have settled more equivalently to the centre point. Significant longitudinal variation of soil properties that would explain the difference in the settlements has not been observed.

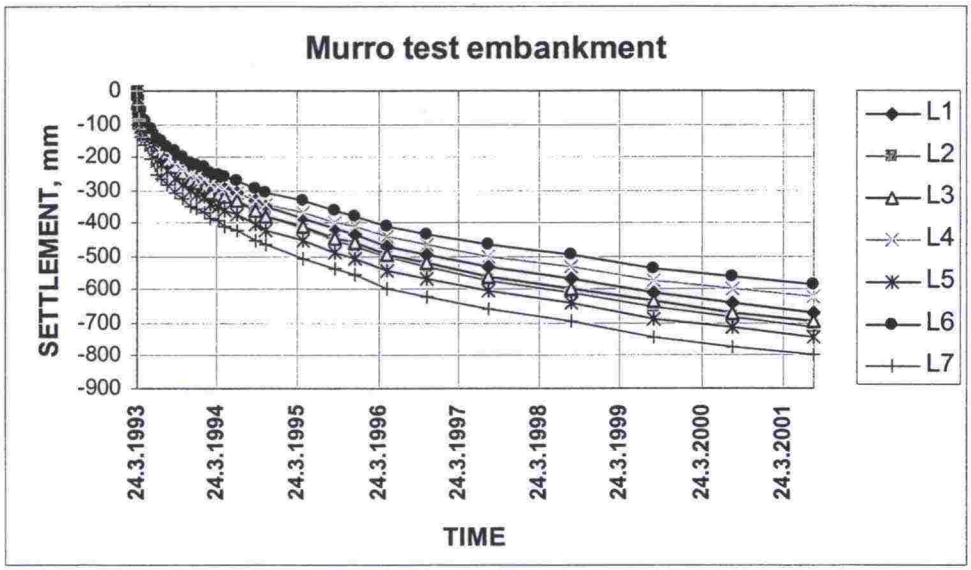

Figure 3.3 Time-settlement graph of Murro test embankment.

The extensometer is located on the centre line of the embankment two meters away from the middle. Settlements at different depths are presented in Figure 3.4. The settlement 1 m below the original ground level corresponds fairly well to the total settlement of the centre point L2. On the basis of Figure 3.3 and Figure 3.4 can be noticed that the total settlement occurs mainly at a depth of 0...8,5 meters, below that no significant settlements have taken place.

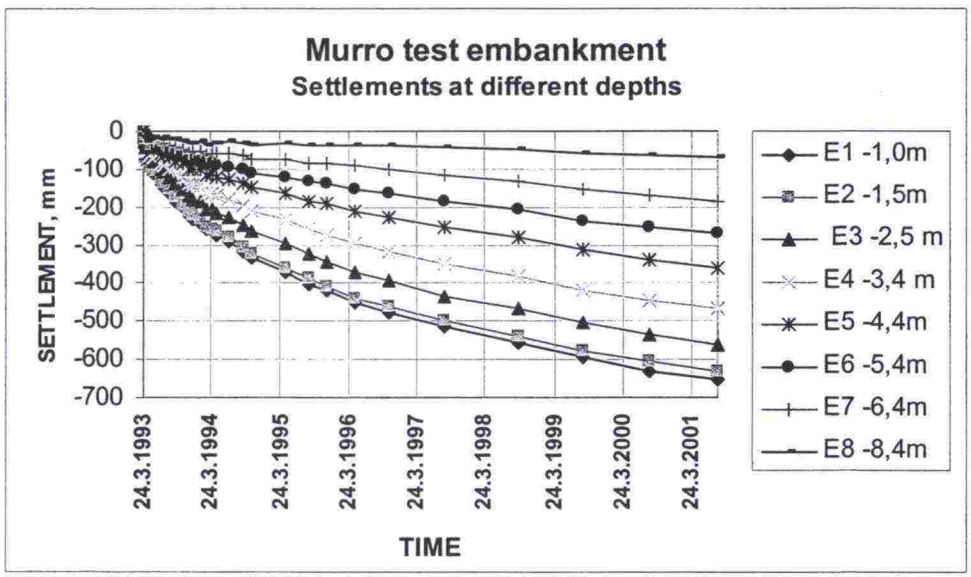

Figure 3.4 Extensometer observations of Murro test embankment.

The horizontal displacements are presented in Figure 3.5 and Figure 3.6. These were measured in two points, on the top and on the bottom of the slope (see Figure 3.1). The maximum displacement can be located at a depth of 4 meters with both inclinometers. The displacement parallel to the embankment is minor according to both inclinometers, and the largest displacement in the perpendicular direction to the embankment is measured at the bottom of the slope. This maximum horizontal displacement is 123 mm, whereas the displacement measured at the top of the slope is 100 mm.

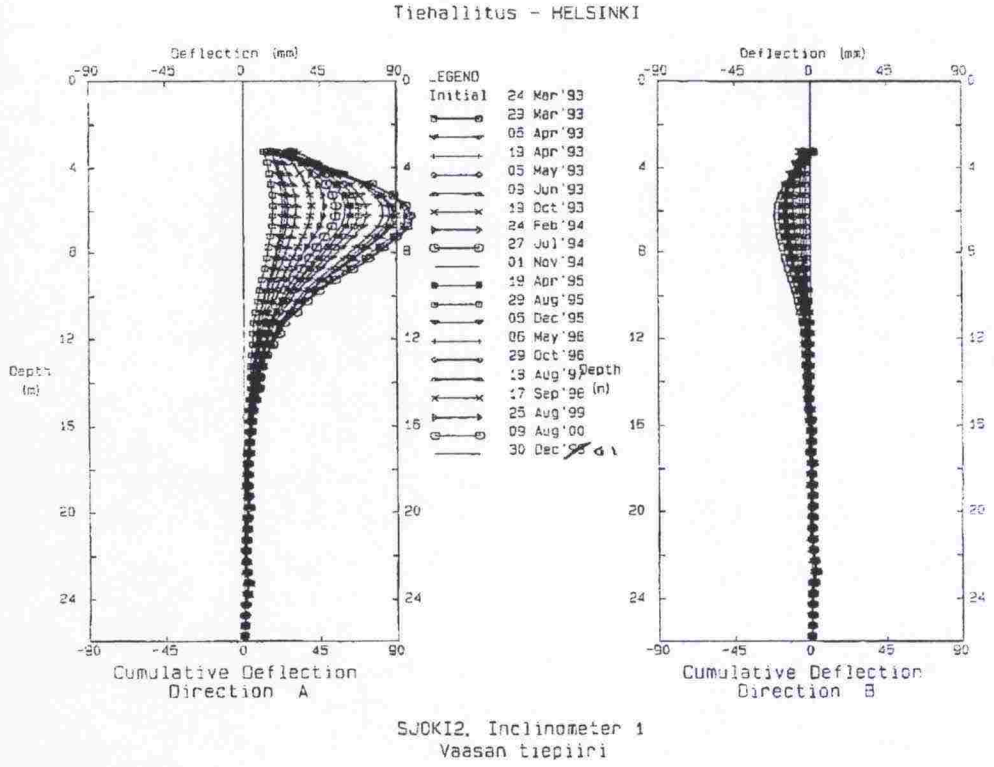

Figure 3.5 *Observations of inclinometer 1 (situated on the edge of the embankment), Murro, Seinäjoki.*

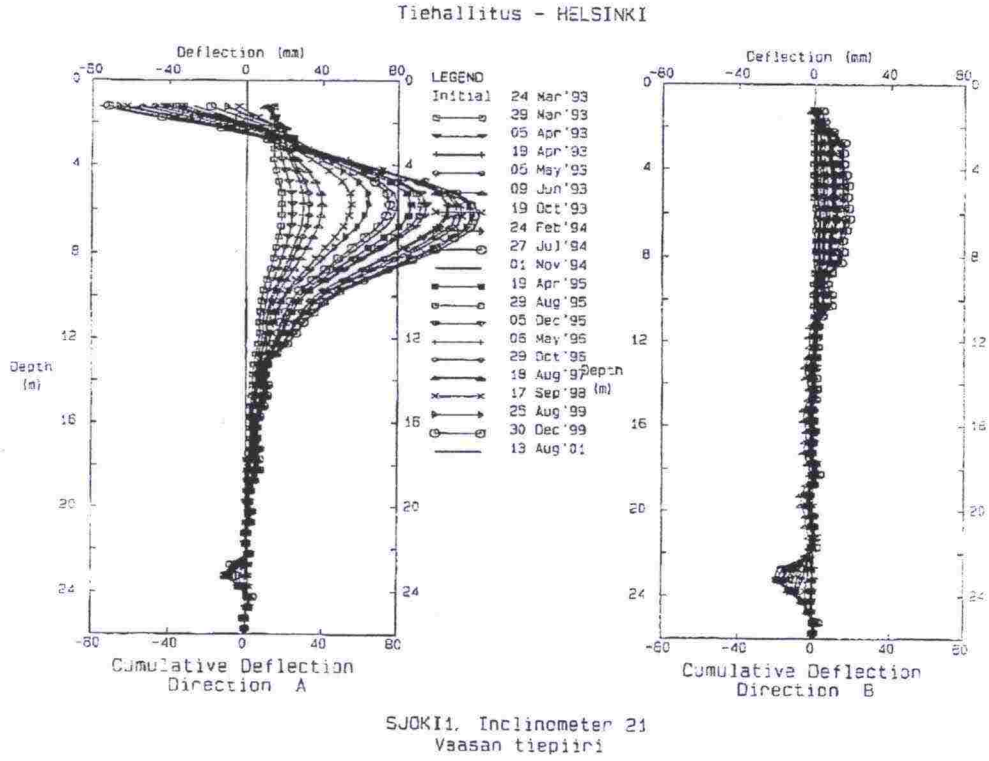

Figure 3.6 *Observations of inclinometer 2 (situated on the bottom of the slope), Murro, Seinäjoki.*

The excess pore pressure observations are presented in Figure 3.7. Some of the latest observations suggest that the excess pore pressure had increased first and then decreased. This hardly is the case and more likely indicates a problem in the measurements.

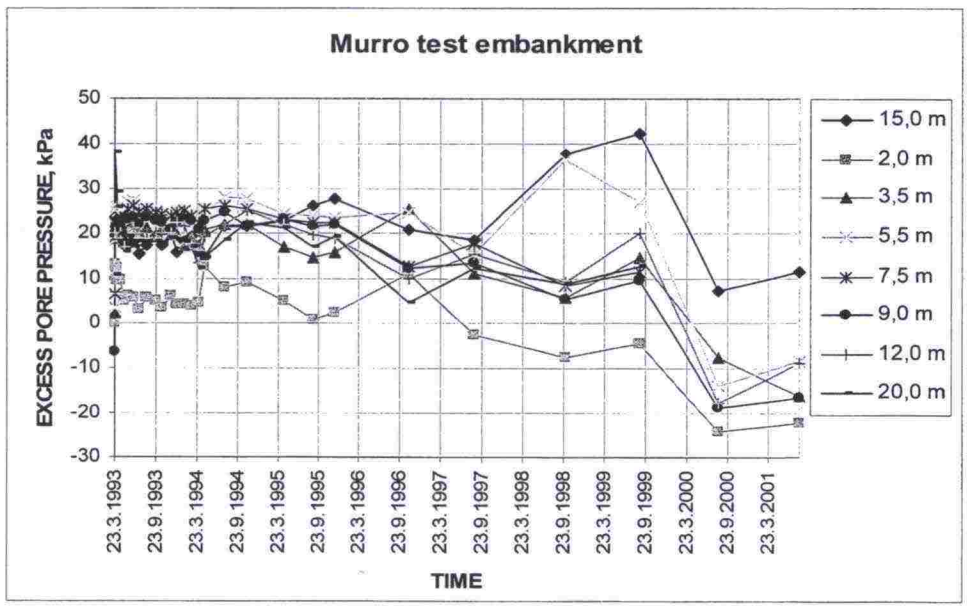

Figure 3.7 *Excess pore pressure observations of Murro test embankment.*

4 SITE INVESTIGATIONS AND LABORATORY TESTS UNDER THE EMBANKMENT

In 2001, additional site investigations were made. This time site investigations were also done under the embankment in order to study the changes that have happened in the soil.

Both disturbed and undisturbed samples were taken. Sampling was done in March and in June. In June, field vane tests, static-dynamic penetration tests and CPTU tests were carried out as well. Laboratory of Soil Mechanics and Foundation Engineering of HUT did most of the sampling and the Finnish Road Administration carried out the other soundings.

Sampling and sounding were done on the natural soil next to the embankment and under the embankment. Samples were taken underneath the centre line of the embankment and from an area that was 13,2 m of the centre line parallel to it. Soundings were done at the maximum 3 m off the centre point of the embankment, and 6 m from the bottom of the slope outside the embankment.

4.1 Site investigations

The results of the site investigations carried out before construction cannot be used as reference material as for static-dynamic penetration tests and cone penetration tests. This is the case because one cannot be sure of the similarity and comparability of the equipment. Development may have happened especially in static-dynamic penetration testing because of the newness of the method. Instead, field vane testing is such a well-established method that those results can be considered to be reliable for studying the changes in the soil during the eight years of consolidation.

The observed groundwater level was 0,80 m below the surrounding ground level measured next to the embankment, and 2,25 m under the embankment level measured on top of it. The embankment itself is two meters thick.

An unexpected phenomenon can be noted in field vane test diagram under the embankment (Figure 4.1) compared to the situation before construction (Figure 2.2a): the shear strength of the lower half of the deposit in the latter case was determined to be about 30 kPa while the more recent diagram would suggest shear strength of only 20 kPa. As for the upper part, a slight increase of the shear strength, about 5 kPa, can be seen.

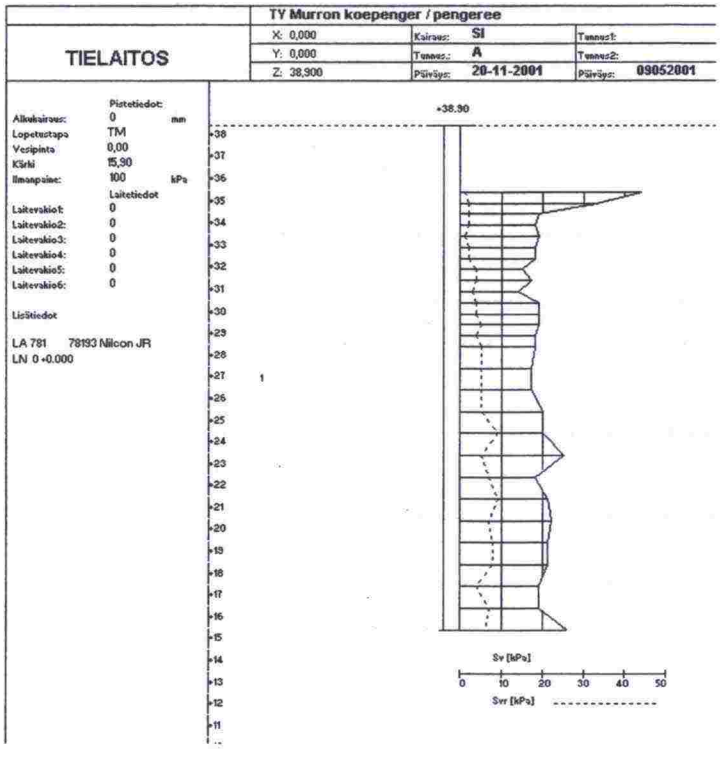

Figure 4.1 *Shear vane test under Murro test embankment eight years after construction.*

Not very clear evidence of changes in the subsoil can be seen when comparing Figure 4.2 to Figure 4.3. They present the results of the static-dynamic penetration tests next to and under the embankment. The traditional CPTU-method shows slight increase in the pore pressure in the upper parts of the deposit, which can be seen in Figure 4.4 and Figure 4.5. A very close inspection shows slight growth of the cone resistance full-length of the sounding in both methods as well as in CPTR tests (Figure 4.6 and Figure 4.7). In CPTR test, the cone penetration test equipment measures resistance as well.

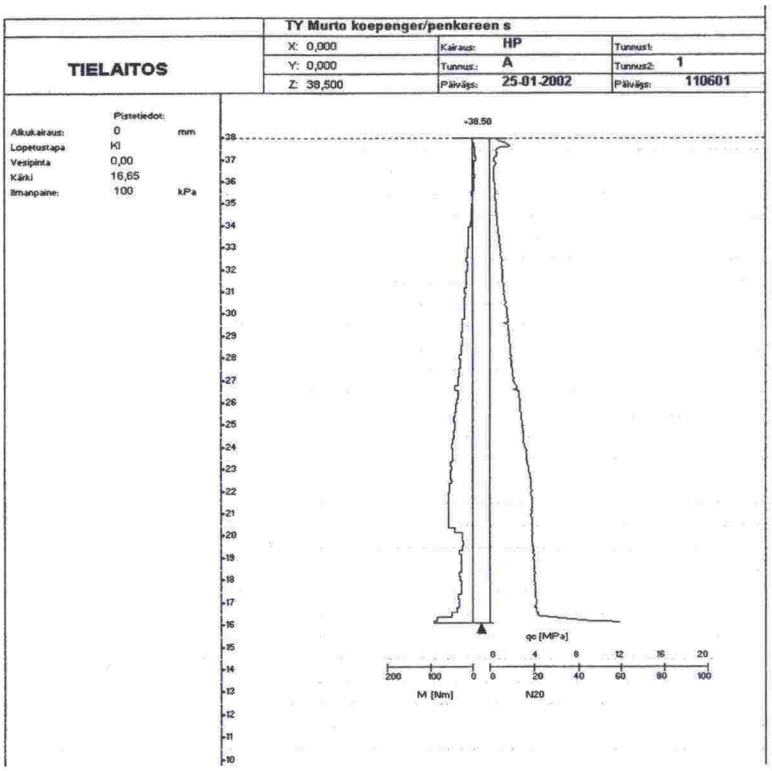

Figure 4.2 Static-dynamic penetration test next to the Murro test embankment.

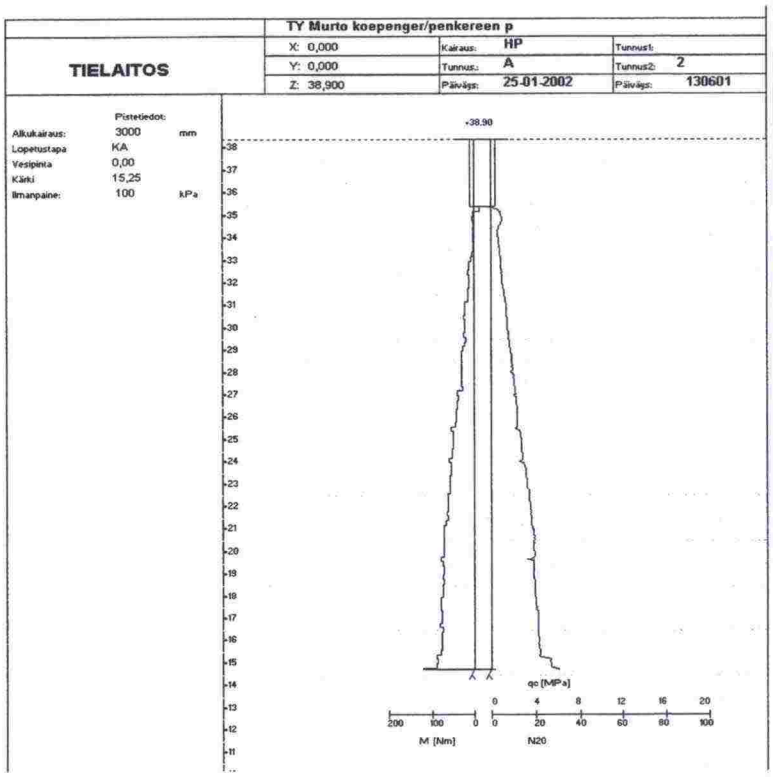

Figure 4.3 Static-dynamic penetration test under the Murro test embankment eight years after construction.

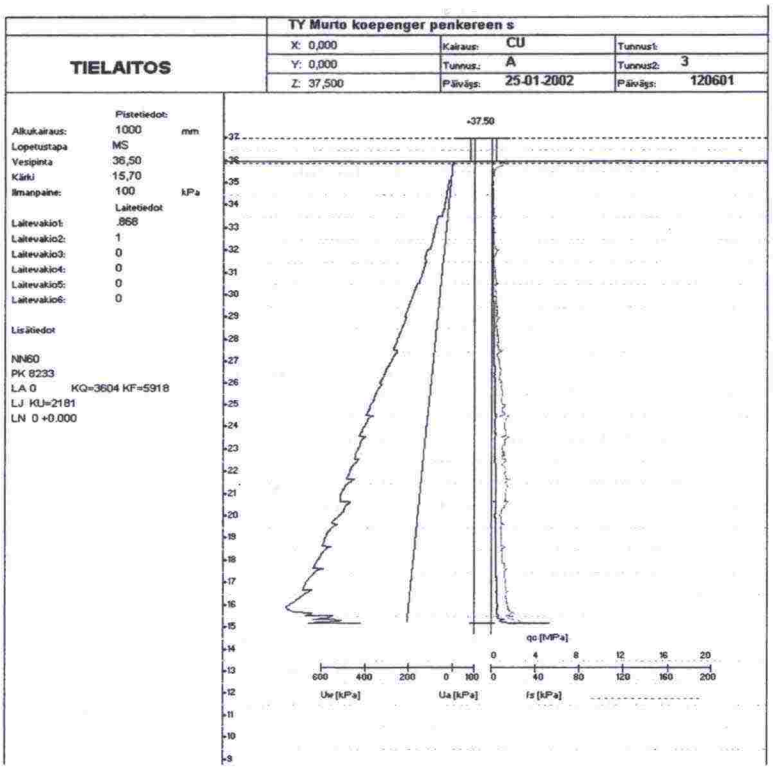

Figure 4.4 CPTU test next to Murro test embankment.

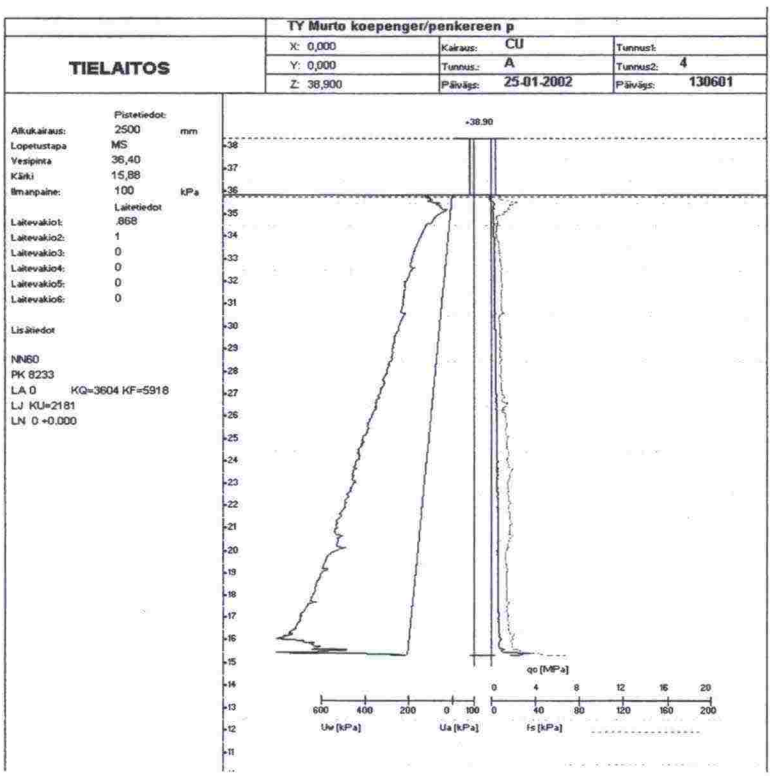

Figure 4.5 CPTU test under the Murro test embankment eight years after construction.

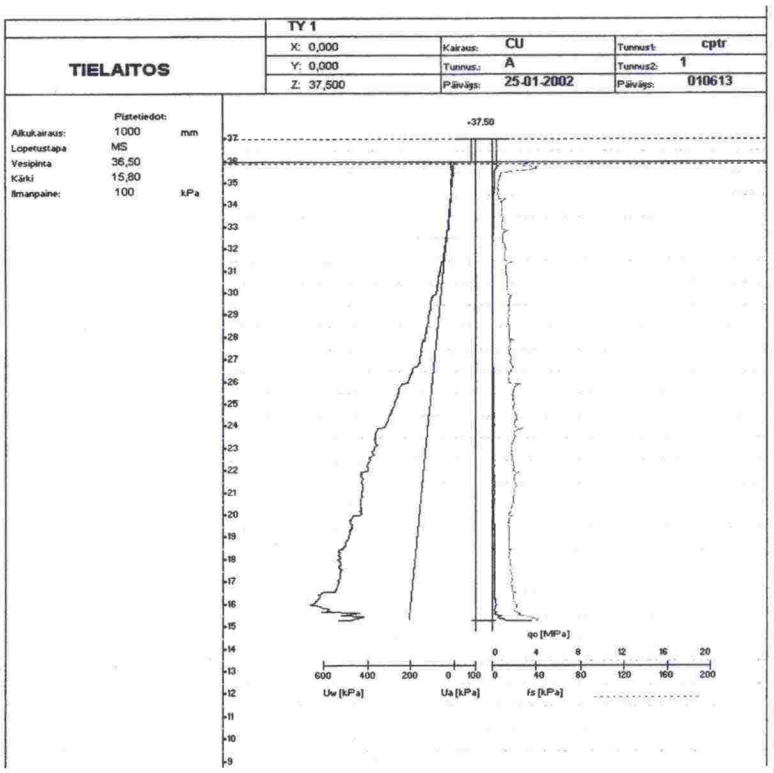

Figure 4.6 CPTR test next to Murro test embankment.

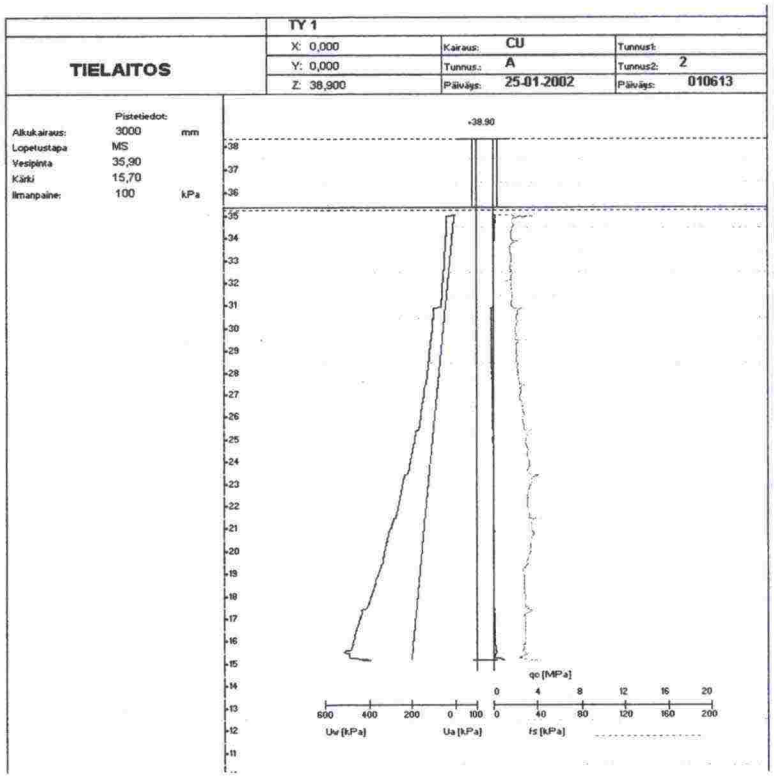

Figure 4.7 CPTR test under Murro test embankment eight years after construction.

4.2 Laboratory tests

Again, a comprehensive series of laboratory tests was made. Soil profiles were determined next to and under the embankment. Determination of index properties and oedometer tests were carried out for the whole layer, and two triaxial test series were done at depths of 4,0-4,5 m and 7,0-7,6 m. The triaxial tests and their results are discussed later on in Section 5.4.

In order to be able to study the changes in the subsoil, the compaction of the soil has to be taken into account. Therefore, the depths of the samples taken under the embankment have been corrected with the help of the extensometer observations to correspond to the depths of natural soil.

Index properties are presented in Figure 4.8. One would expect to discover changes in water content, unit weight, void ratio and shear strength from the fall cone test. These changes can be observed in some extent as well. The changes have happened mainly in the softest layer, 2-8 m. The water content has decreased with about 30 percent at the maximum and the unit weight has increased slightly at the same time.

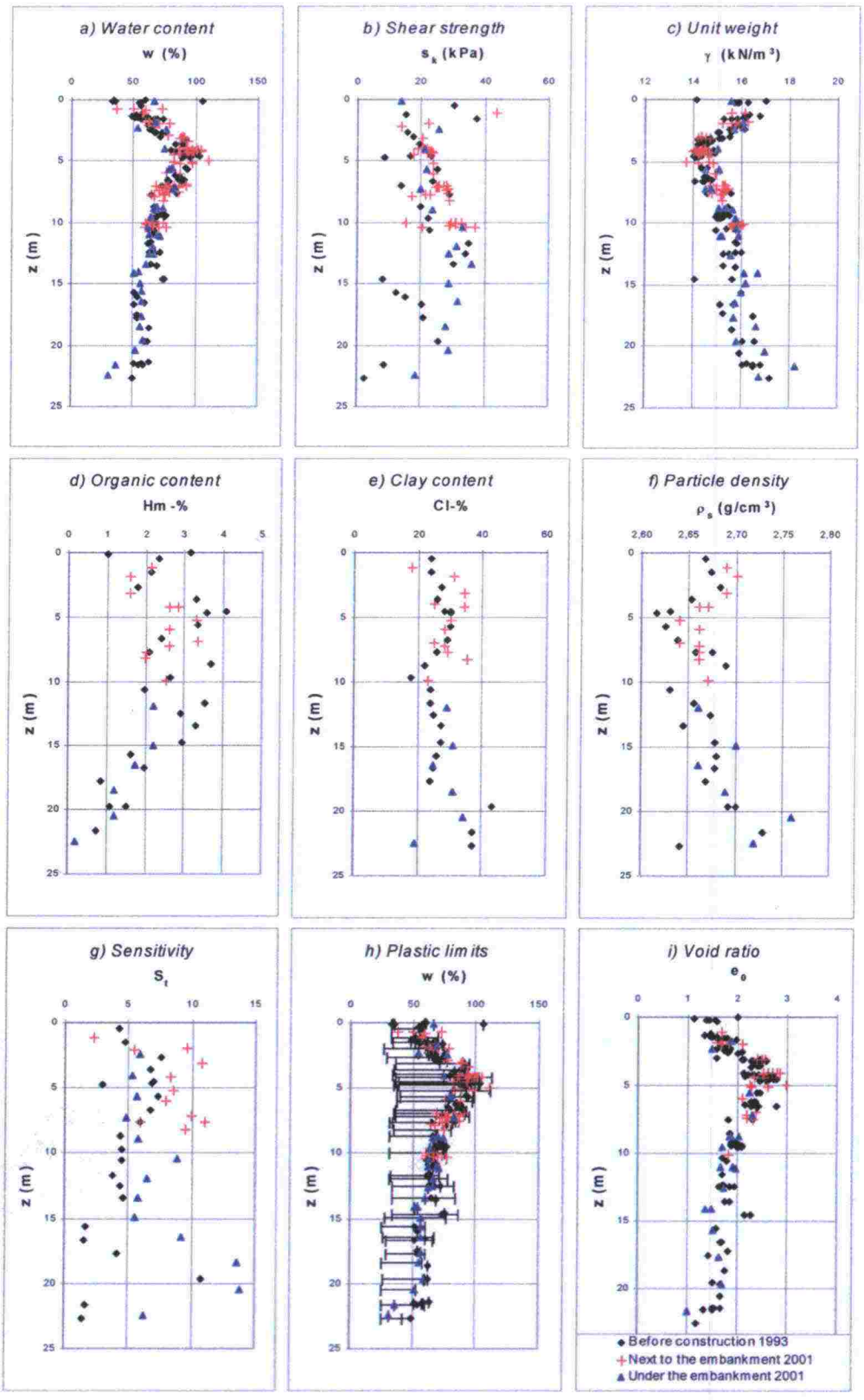

Figure 4.8 Index properties of Murro clay.

The changes in oedometer test results presented in Figure 4.9 are very small. The small increase of the normal consolidated modulus number and stress exponent are the most prominent. The value of the stress exponent has shifted towards zero as for the first ten meters. The stress exponent β of a disturbed sample is usually close to zero as well. The ratio of normal and overconsolidated modulus numbers is about ten.

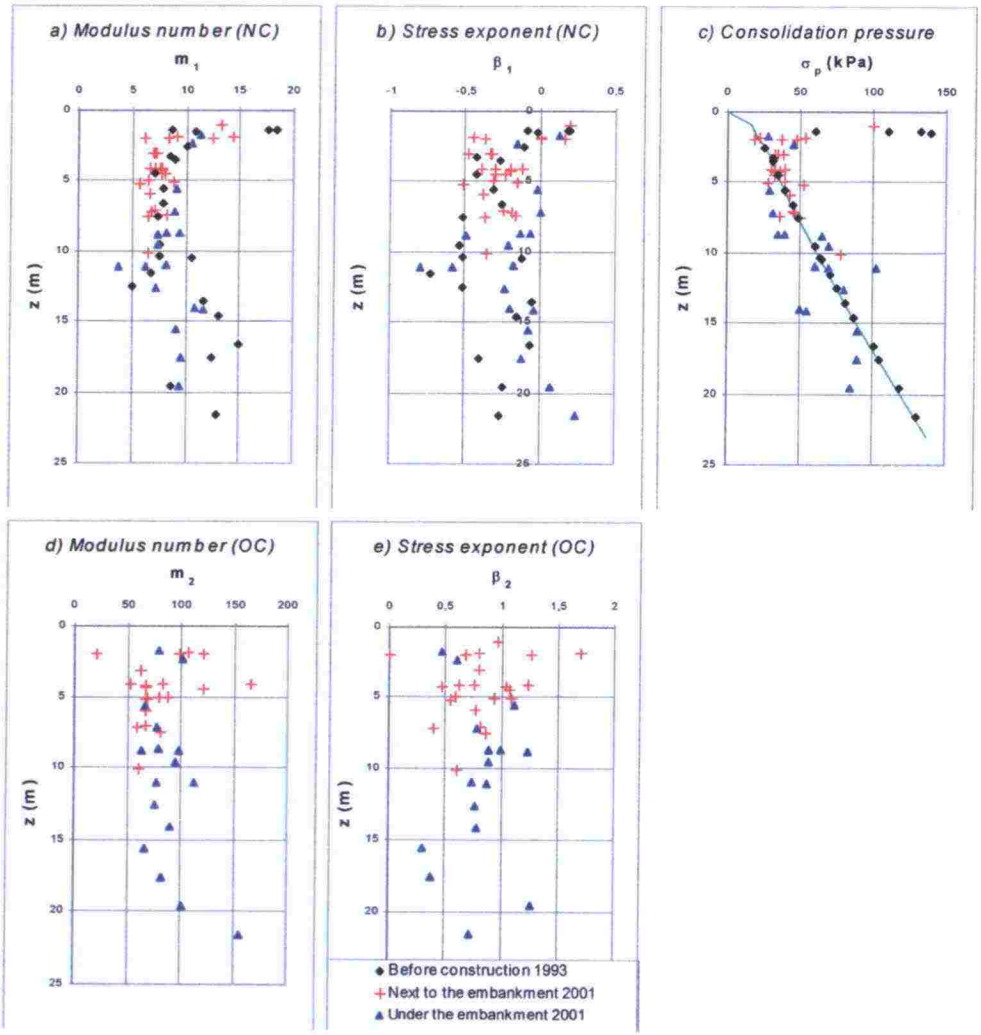

Figure 4.9 Summary of oedometer test results of Murro clay.

5 MODEL COMBINING ANISOTROPY AND DE-STRUCTURATION

5.1 Background

There is often a degree of structure present in natural soils. In fact, soft soil without structure is an exception. Structure consists of two elements: fabric and interparticle bonding. Fabric means the texture of soil, i.e. the arrangement of particles and particle contacts. One demonstration of fabric is the anisotropy of natural soils. Anisotropic microstructure of clay results from the asymmetric shape of clay platelets, sedimentation and consolidation process. The bonding between the particles is cohesive by nature and it increases the strength of the soil compared to unstructured soil. Bonding is demonstrated for example by the sensitivity of soil.

The evolution of structure is a very long-term process. For many Finnish clays the development of structure has taken place since the last Ice Age because of various reasons.

Loading induces changes in structure. When the deformations are elastic and recoverable, loading does not damage the structure. When the yield stresses are exceeded and the deformations become irrecoverable (plastic), the particles start to re-arrange themselves and the mineral platelets start to slip past one another, and therefore, the bonding starts to rupture. This phenomenon is called de-structuration. The slippage happens gradually so that in a triaxial test natural material has a compression line that curves towards the compression line of an unstructured material. The difference between the curves is a demonstration of bonding. This is indicated schematically in Figure 5.1. The properties of unstructured soil are called intrinsic properties in order to distinguish them from the properties of natural soil.

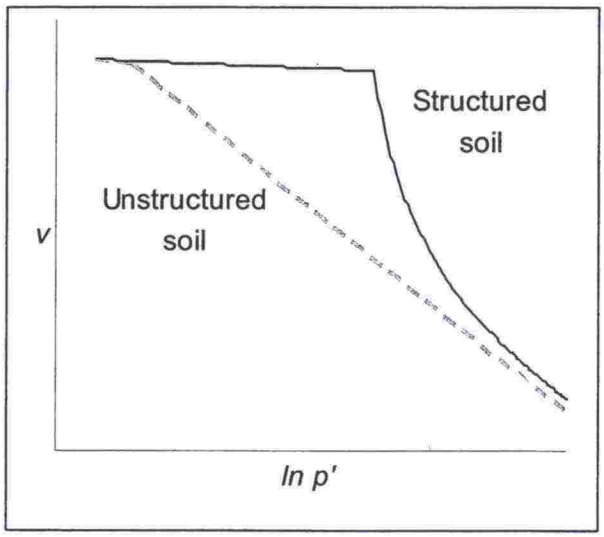

Figure 5.1 The behaviour of structured and unstructured clay.

In most of the most advanced constitutive models for soft soil, only one element of structure is taken into account but usually not both of them. The models also tend to be very complicated. Therefore, there was a need for a relatively simple model that combines anisotropy and de-structuration. A new soil model for soft, normally or lightly overconsolidated soils, referred here as SS-CLAY1 and sometimes also referred as DS-CLAY1 (Wheeler 2001), was developed at University of Glasgow in collaboration with Helsinki University of Technology. It is an extension to a previous model called S-CLAY1, which describes the anisotropy of plastic behaviour with a rotational component of hardening. These models have been embedded in an elasto-plastic framework similarly to the critical state models.

5.2 Model formulation

In triaxial space the stress state is described with deviator stress q and mean effective stress p', defined as:

$$q = \sigma'_1 - \sigma'_3 \tag{5.1}$$

$$p' = \frac{1}{3}(\sigma'_1 + 2\sigma'_3) \tag{5.2}$$

where σ'_1 and σ'_3 are the principal effective stresses.

Because plastic deformations are assumed to be dominating, elastic behaviour of soil is for simplicity thought to be isotropic and is described by the same elastic relationship as in Modified Cam Clay (Roscoe & Burland 1968):

$$\begin{bmatrix} d\varepsilon_v^e \\ d\varepsilon_d^e \end{bmatrix} = \begin{bmatrix} \frac{\kappa}{vp'} & 0 \\ 0 & \frac{1}{3G'} \end{bmatrix} \begin{bmatrix} dp' \\ dq \end{bmatrix} \tag{5.3}$$

where $d\varepsilon_v^e$ is the increment of elastic volumetric strain, $d\varepsilon_d^e$ is the increment of elastic deviatoric strain, v is the specific volume, κ is the slope of the swelling line in ln p':v plane and G' is the effective shear modulus.

The yield function of the model is a sheared ellipse (Korhonen and Lojander 1987, Dafalias 1987). It is defined in triaxial space by

$$f = (q - \alpha p')^2 - (M^2 - \alpha^2)(p'_m - p')p' = 0 \tag{5.4}$$

where M is the value of the stress ratio η=q/p' in critical state, p'_m defines the size of the yield curve and α defines the inclination of the yield curve. Because structure gives the soil extra strength, the yielding of unstructured soil happens prior to the yielding of structured, natural soil. Therefore, two yield curves are needed: initial yield curve for natural soil and a smaller intrinsic yield curve for unstructured soil. The shape of these curves is assumed to be the same, suggesting the same values for the critical state parameter M and the inclination α of the curves. The difference between the sizes of the curves describes the amount of bonding between the clay particles. It is described by parameter x so that the relationship between the sizes of the curves is

$$p'_m = (1 + x)p'_{mi} \tag{5.5}$$

The curves are presented in Figure 5.2.

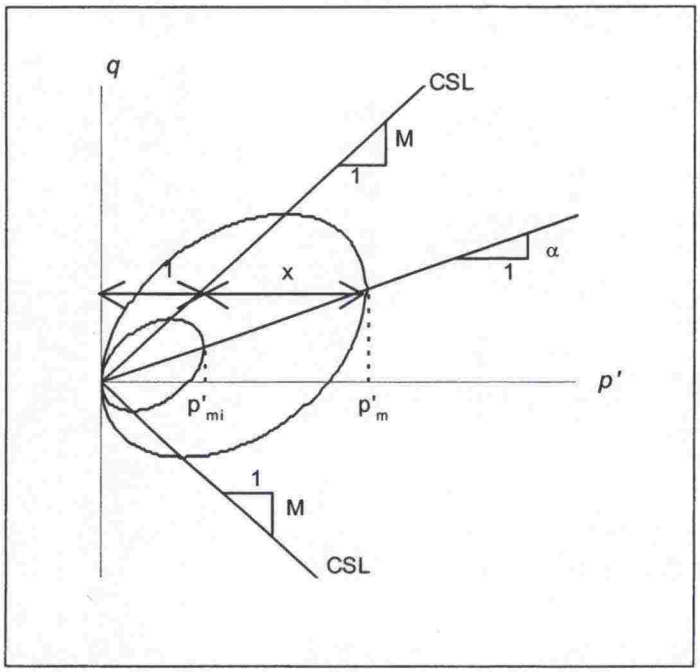

Figure 5.2 Yield curves of SS-CLAY1 model.

In SS-CLAY1, there are four hardening laws: two considering changes in sizes of the yield curves (Equations 5.6 and 5.7), a rotational hardening law (Equation 5.8) and the law controlling the degradation of the bonding effect (5.9).

$$dp'_{mi} = \frac{vp'_{mi}}{\lambda - \kappa} d\varepsilon^{p}_{v} \tag{5.6}$$

$$dp'_{m} = p'_{mi}\, dx + dp'_{mi}\,(1 + x + dx) \tag{5.7}$$

$$d\alpha = \mu\left[\left(\frac{3\eta}{4} - \alpha\right)\left\langle d\varepsilon^{p}_{v}\right\rangle + \beta\left(\frac{\eta}{3} - \alpha\right)\left|d\varepsilon^{p}_{d}\right|\right] \tag{5.8}$$

$$dx = a\left[(0 - x)\left|d\varepsilon^{p}_{v}\right| + b(0 - x)\left|d\varepsilon^{p}_{d}\right|\right] = -ax\left(\left|d\varepsilon^{p}_{v}\right| + b\left|d\varepsilon^{p}_{d}\right|\right) \tag{5.9}$$

Equation (5.6) is analogous to the hardening law of Modified Cam Clay. Parameter λ is the slope of the normal consolidation line in ln p':v plane of the reconstituted soil (intrinsic property). The two other hardening laws have similarities, so that parameters μ and a are absolute rate parameters controlling hardening, and constants β and b control the relative effectiveness of plastic volumetric and plastic deviatoric strains in the hardening process. The target values of the inclination depend on the stress path and the target value for the de-structuring is zero.

An associated flow rule is assumed, so plastic strains are

$$d\varepsilon_v^p = \Lambda \frac{\partial g}{\partial p'} \tag{5.10}$$

$$d\varepsilon_d^p = \Lambda \frac{\partial g}{\partial q} \tag{5.11}$$

where g=f is the plastic potential function and Λ is the plastic multiplier. The equations above result to a plastic compliance matrix

$$\begin{bmatrix} d\varepsilon_v^p \\ d\varepsilon_d^p \end{bmatrix} = \frac{1}{H} \begin{bmatrix} \frac{df}{dp'}\frac{df}{dp'} & \frac{df}{dq}\frac{df}{dp'} \\ \frac{df}{dp'}\frac{df}{dq} & \frac{df}{dq}\frac{df}{dq} \end{bmatrix} \begin{bmatrix} dp' \\ dq \end{bmatrix} \tag{5.12}$$

where the hardening modulus H, based on the standard elasto-plastic procedure, is

$$H = -\left[\frac{\partial f}{\partial p'_{mi}} \frac{\partial p'_{mi}}{\partial \varepsilon_{vp}} \frac{\partial f}{\partial p'} + \frac{\partial f}{\partial x} \left(\frac{\partial x}{\partial \varepsilon_v^p} \left| \frac{\partial f}{\partial p'} \right| + \frac{\partial x}{\partial \varepsilon_d^p} \left| \frac{\partial f}{\partial q} \right| \right) + \frac{\partial f}{\partial \alpha} \left(\frac{\partial \alpha}{\partial \varepsilon_v^p} \left\langle \frac{\partial f}{\partial p'} \right\rangle + \frac{\partial \alpha}{\partial \varepsilon_d^p} \left| \frac{\partial f}{\partial q} \right| \right) \right] \tag{5.13}$$

5.3 Parameter determination

The total number of parameters in SS-CLAY1 is ten. Four are the same as in Modified Cam Clay: κ, M, G', and v. The slope λ of the normal consolidation line differs from the one in MCC model so that in SS-CLAY1 the intrinsic value is used. All these can be determined from conventional laboratory tests.

The initial state, namely the sizes and inclination of the yield curves, can be determined from triaxial tests. The inclination is a function of the friction angle, and the method for calculating it was presented by Wheeler et al. (1999). The size of the initial yield curve can be fitted to observations. The relative difference x_0 between the sizes of the two yield curves can be chosen on the basis of the sensitivity of the soil, or preferably by calculating it from the position of the yield point relative to the intrinsic compression line (Wheeler 2001).

Wheeler et al. (1999) presented also a methodology for calculating the initial value of soil constant β from the friction angle. While there is no direct way to

determine constant μ experimentally, it can be estimated to be of the order of $10/\lambda$ to $15/\lambda$ of natural clay.

The determination of parameters a and b, due to the very early stage of the model development, require test simulations. The range of these parameters based on test data from POKO clay was found to be a=1...2 and b=2...5 (Koskinen 2001).

5.4 Test results

Two series of triaxial tests were carried out in order to study the behaviour of Murro clay with the model SS-CLAY1. The tests were performed on samples from boreholes next to the embankment and the sampling was done in 2001. First series was from a depth of 4,0-4,5 m, and the second from a depth of 7,0-7,6 m. Both series included one shear test and four consolidation tests at the minimum. The tests and short descriptions are presented in Table 5.1.

The tests were studied with the intention of determining the initial yield curves. The yield points of the first series fitted well to the proposed yield curve, which is presented in Figure 5.3. Value of the critical state parameter M was determined from the shear test and the inclination α of the curve was calculated based on it. The size of the curve was fitted to match the observed yield points.

On the basis of the shear test, the same value of the critical state parameter M was found to be convenient for the second series as well. The proposed yield curve is presented in Figure 5.4. The yield points fit to the curve in this case as well.

Table 5.1 Test series on Murro clay in 2001.

	Test	Depth m	Bore-hole	η_1	p'_{1max} kPa	q_{1max} kPa	η_2	p'_{2max} kPa	q_{2max} kPa
Series 1	CAD 3033	4,04-4,15	2001-3	0,92	86,7	80,0	0,058	214	12,9
	CAD 3074	4,00-4,11	2001-8	0,98	74,5	73,4	0,098	206	18,5
	CAE 3071	4,02-4,13	2001-9	-0,40	79,4	-31,8	0,60	193	97,5
	CAD 3090	4,02-4,13	2001-7	0,06	102	6,5	1,18	167	200
	CAE 3079	4,19-4,30	2001-8	0,50	78,1	39,4	-0,65	145	-106
	CAD 3080	4,36-4,47	2001-8	0,31	77,8	23,4	1,12	205	225
	CADC 3013	4,48-4,37	2001-3	Shear	-	-	-	-	-
Series 2	CAE 2990	7,04-7,15	2001-2	-0,65	61,3	-41,0	0,58	131	77,2
	CAE 2989	7,15-7,26	2001-2	0,61	75,5	46,4	-0,66	122	-83,6
	CAD 2987	7,26-7,37	2001-2	0,20	75,1	15,2	0,87	127	111
	CAD 2988	7,37-7,48	2001-2	0,91	85,9	77,8	0,05	168	9,0
	CADC 2986	7,51-7,63	2001-2	Shear	-	-	-	-	-

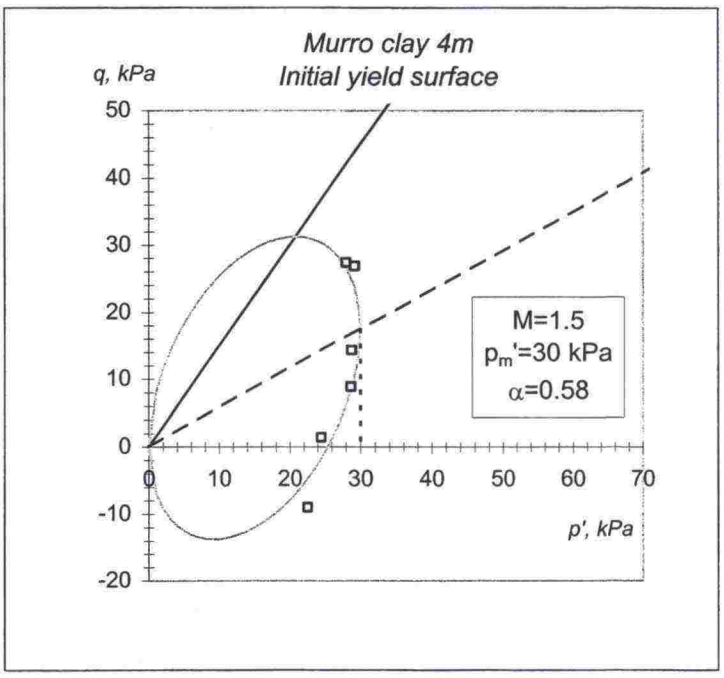

Figure 5.3 Initial yield curve of Murro clay from a depth of 4,0-4,5 m.

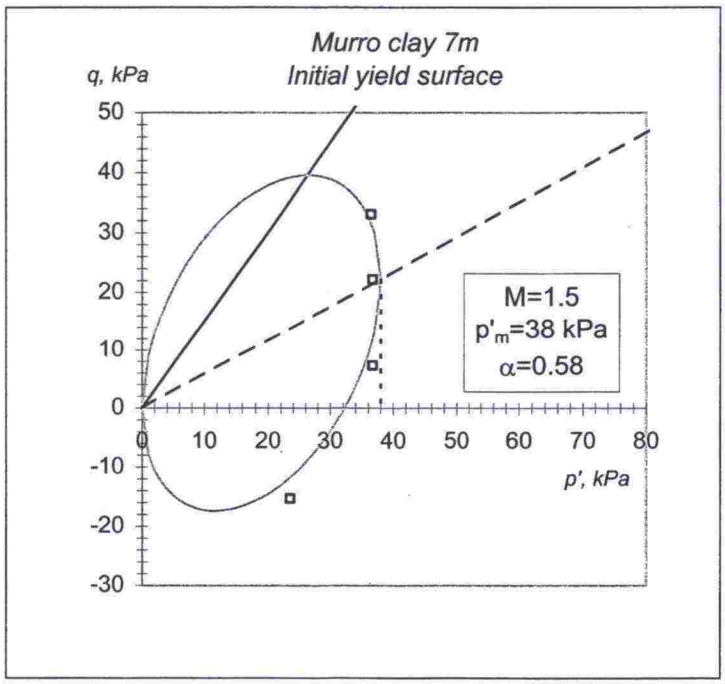

Figure 5.4 Initial yield curve of Murro clay from a depth of 7,0-7,6 m.

6 RESULTS OF THE CALCULATIONS

6.1 Calculations with PLAXIS

6.1.1 Initial data

The width of the upper part of the test embankment is 10,0 meters and the height from the ground level is 2,0 meters. There is a 1,6 meters thick heavily overconsolidated layer under the embankment, which was modelled in the PLAXIS-calculations with the ideally elasto-plastic Mohr-Coulomb material model (MC model). The soft clay layers below that were modelled with the Soft Soil model (SS model). The failure and yield surfaces of the Soft Soil –model are presented in Figure 6.1: the failure surface is formed according to the Mohr-Coulomb failure criteria and the yield surface (cap) according to the Modified Cam Clay –model that includes cohesion.

The layers and their parameters are presented in Tables 6.1...6.4.

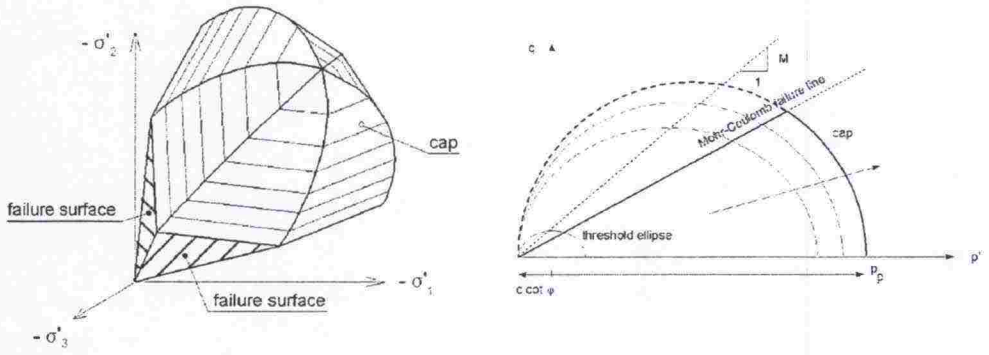

Figure 6.1 *The failure and yield surface of SS model: on the left in three-dimensional principal stress space and on the right in the co-ordinate system of mean effective stress p' and deviator stress q. M is the slope of the critical state line, p'_p is the effective consolidation stress on the hydrostatic axis.*

Table 6.1 *The layers and overconsolidation conditions used in PLAXIS.*

Layer number	Soil type	Depth, m	Material model	POP, kPa
1	Clay (OC)	0,0-1,6	MC	Not used
2	Clay (NC)	1,6-3,0	SS	0
3	Clay (NC)	3,0-6,7	SS	0
4	Clay (NC)	6,7-10,0	SS	0
5	Clay (NC)	10,0-15,0	SS	0
6	Clay (NC)	15,0-23,0	SS	0
7	Embankment	-	MC	Not used

Table 6.2 Parameters of the Soft Soil –model, part 1.

Layer number	γ_{dry} kN/m^3	γ_{wet} kN/m^3	k_x m/day	k_y m/day	c_k -	λ^* -	κ^* -
2	15,6	15,6	$6{,}22*10^{-4}$	$4{,}75*10^{-4}$	0,7	0,143	0,0107
3	14,5	14,5	$5{,}18*10^{-4}$	$3{,}89*10^{-4}$	1,1	0,143	0,0103
4	15,1	15,1	$3{,}20*10^{-4}$	$2{,}59*10^{-4}$	0,8	0,129	0,0097
5	15,5	15,5	$1{,}99*10^{-4}$	$1{,}56*10^{-4}$	0,7	0,136	0,0121
6	16,0	16,0	$3{,}02*10^{-4}$	$2{,}33*10^{-4}$	0,7	0,054	0,0015

Table 6.3 Parameters of the Soft Soil –model, part 2.

Layer number	ν_{ur} -	K_0^{NC} -	c' kN/m^2	φ' °	ψ °	e_{init} -
2	0,35	0,7	2	37	0	1,8
3	0,10	0,7	3	37	0	2,5
4	0,15	0,7	0	37	0	2,1
5	0,15	0,7	0	37	0	1,8
6	0,15	0,7	0	37	0	1,6

Table 6.4 Parameters of the Mohr-Coulomb model.

Layer number	γ_{dry} kN/m^3	γ_{wet} kN/m^3	k_x m/day	k_y m/day	ν -	E MPa	c' kPa	φ' °	ψ °
1	16,2	16,2	$6{,}22*10^{-4}$	$4{,}75*10^{-4}$	0,35	11,3	2	39,2	0
Embank-ment	19,6	19,6	1	1	0,35	40	2	40	0

Parameters presented in previous tables (PLAXIS manual, version 7, 1998):

γ_{dry} Total unit weight of soil above the groundwater level

γ_{wet} Total unit weight of soil below the groundwater level

k_x Horizontal permeability in initial state ($=k_{0x}$)

k_y Vertical permeability in initial state ($=k_{0y}$)

ν, ν_{ur} Poisson ratio. MC: first loading; SS: unloading/reloading

E Young's modulus (MC)

c Cohesion

φ Friction angle

ψ Dilatancy angle

λ^* Modified compression index, NC (SS)

κ^* Modified swelling index, OC (SS)

c_k Factor of change of permeability

The overconsolidation conditions are characterised with parameter POP in Equation (6.1).

$$POP = \sigma_c - \sigma_{yy}^0 \geq 0 \tag{6.1}$$

where σ_c is the consolidation stress and σ_{yy}^0 the current effective vertical stress. The decrease of the permeability is considered as presented in Equation (6.2).

$$\lg\left(\frac{k}{k_0}\right) = \frac{\Delta e}{c_k} \tag{6.2}$$

where k is the changed permeability and Δe is the change of the void ratio during consolidation.

15-node triangle elements were used in the calculations. When creating the element mesh, symmetry of the embankment was not used (see Appendix 1). The boundary conditions of consolidation were open at the ground surface, on the bottom of the mesh and on both sides during the consolidation stage.

The following modelling order was used:

1. Calculation of the initial stresses.
2. Adding the load of the embankment in two stages under undrained conditions.
3. Calculation of the consolidation stage.

6.1.2 Results of the calculations

In this section the settlements, pore pressures and horizontal displacements calculated with the program PLAXIS are studied. In addition, the evolution of plastic points in the subsoil and the evolution of stress paths and the undrained shear strength are examined in the subsoil under the centre line of the embankment during the consolidation process.

In Appendix 1, the deformed element mesh after 8 years of consolidation is presented. The calculated settlement corresponding to this moment is 76 cm.

Figure 6.2 presents the settlement of the ground below the centre line of the embankment in logarithmic time scale. The calculated settlement is com-

pared with the observed one, and the match is rather good at the end. The primary consolidation process seems still to be going on for a few years, and the secondary consolidation will become marked after 30 years from the construction.

The calculated time-settlement behaviour of the subsoil under the centre line of the embankment is presented in Figure 6.3 in linear time scale until eight years. The settlement of the overconsolidated layer (MC model) is minimal. Most of the settlements have happened in layers 2 and 3.

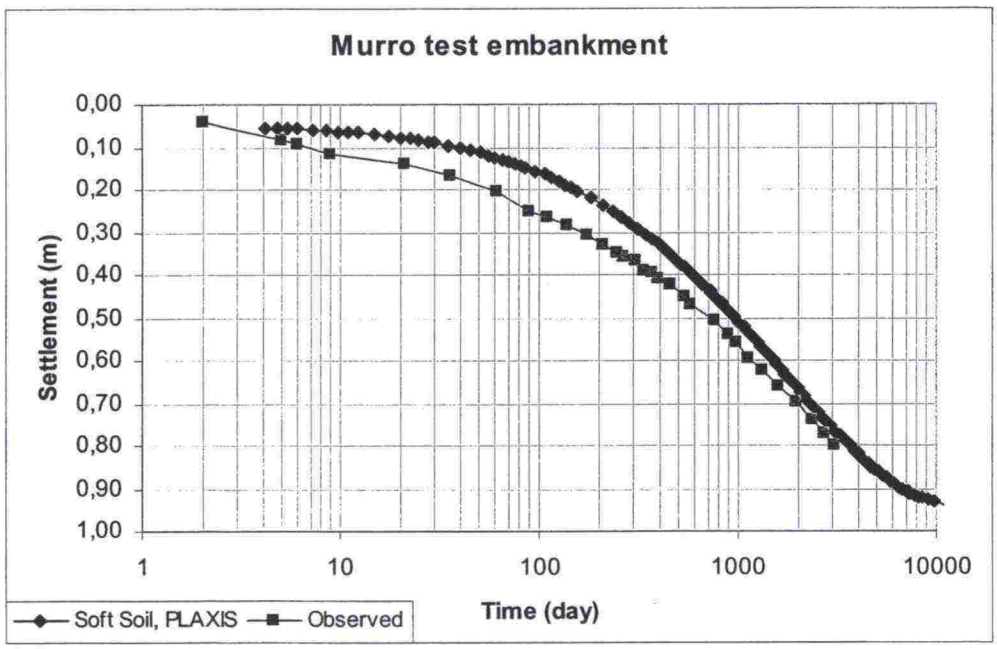

Figure 6.2 *The settlement of the ground below the centre line of Murro test embankment in logarithmic time scale. The observed and the calculated values are compared.*

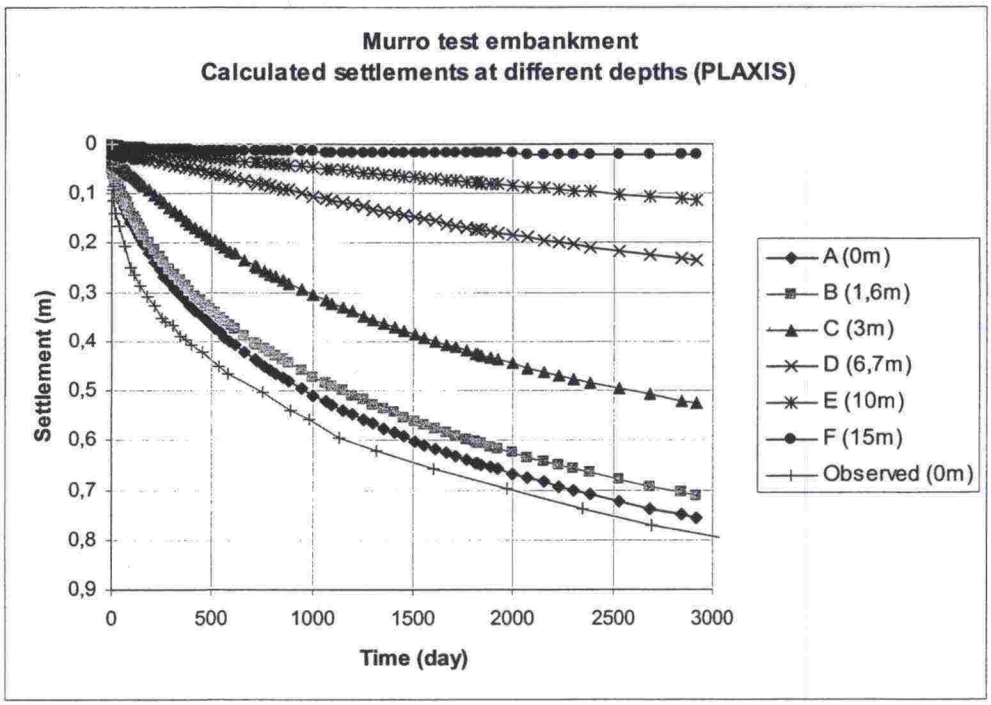

Figure 6.3 *The time-settlement behaviour of different soil layers below the centre line of the Murro test embankment in linear time scale.*

In Appendix 2a, the distribution of the excess pore pressures at the end of the construction is presented. The excess pore pressures are concentrated in layers 2 and 3, where the calculated maximum pressure is 40,1 kPa. After eight years, the location of the maximum pore pressure has gone down to the boundary of layers 4 and 5. The calculated maximum value is then 8,7 kPa.

Appendix 3 shows the horizontal displacements eight years after the construction. The calculated displacements concentrate underneath the slopes approximately 2 meters below the ground surface. The maximum displacement that was calculated was 10,6 cm. The observed maximum displacement 12,3 cm is located slightly deeper instead. The development of both calculated and observed maximum horizontal displacements with time is presented in Figure 6.4. For two years the calculated and observed values are very close to each other, but after that the calculated curve falls below the observed one.

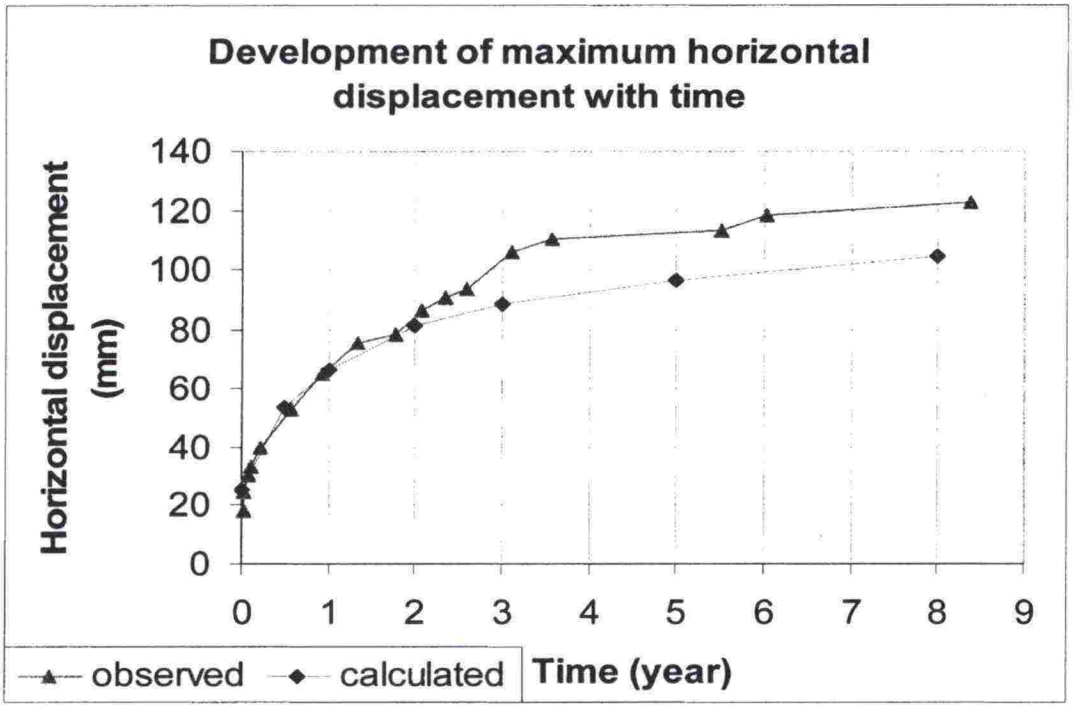

Figure 6.4 *Calculated (with PLAXIS, Soft Soil model) and observed maximum horizontal displacements of Murro test embankment.*

The plastic points in the subsoil and in the embankment eight years after construction are shown in Appendix 4. Plastic points cover all the subsoil, which is believable because the subsoil is considered normally consolidated.

The stress paths can be calculated with the help of the mean effective stress p' and deviator stress q. The stress paths are presented in Figure 6.5, and the depths of the stress points are told in Table 6.5.

Table 6.5 *The depths of the stress path points below the centre line of Murro test embankment.*

Point	Layer number	Depth, m
H	2	2,1
I	3	4,1
J	4	7,7
K	5	11,5
L	6	18,5

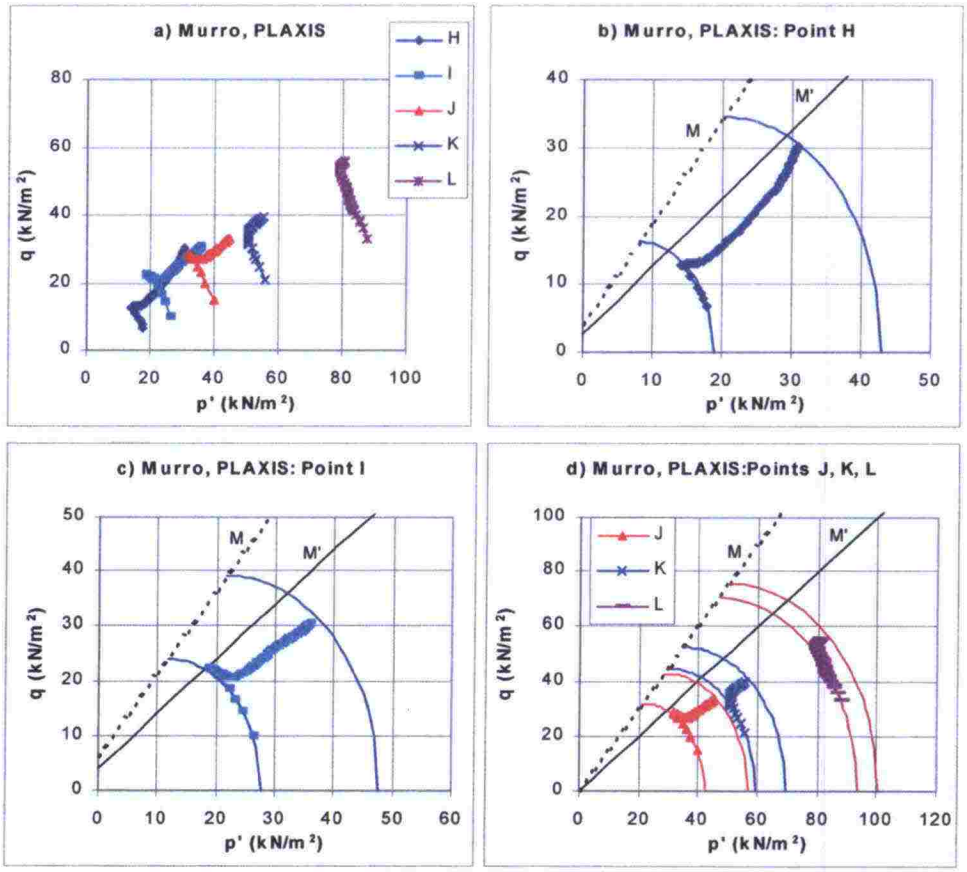

Figure 6.5 *The calculated stress paths in points H, I, J, K and L, the corresponding failure lines M' and critical state lines M.*

Figure 6.5 shows also the failure lines of each stress path point calculated with the help of the corresponding effective strength parameters. The slope of the failure line is smaller than the slope of the critical state line M of PLAXIS. The slope of the failure line is then marked with M' and the cohesion term with N'. The equation of the failure line can then be formularised with Equation (6.3). In plane strain condition M' can be approximated with Equation (6.4) and N' with Equation (6.5).

$$q = M' p' + N' \tag{6.3}$$

$$M' = \frac{6 \sin \varphi}{3 + \sin \varphi} \tag{6.4}$$

$$N' = \frac{6c \cos \varphi}{3 + \sin \varphi} \tag{6.5}$$

In Equations (6.3) to (6.5), the compression stresses are positive. It should be noticed that there is a plus sign in the nominator of Equations (6.4) and (6.5), whereas there is a minus sign on analysing a triaxial test.

It can be noticed from Figure 6.5, that the stress paths start from the K_0-line, bump into the failure line, and then climb up approximately along it.

The growth of the undrained shear strength of the soil in the stress points during the consolidation process is normally evaluated with an equation suggested by Wood (1990). This equation is in the critical state model Modified Cam Clay, and it is based on the growth of the yield surface (cap) and the consolidation stress. As for the SS model in PLAXIS, this method is questionable, because the slope of the failure line is smaller than the slope M of the critical state. The consolidation stress and the corresponding undrained shear strength can be calculated from Equations (6.6) to (6.8), when the extra terms that follow from cohesion are added to Wood's original model (see Figure 6.1).

$$a = c \cot \varphi \tag{6.6}$$

$$p'_c = \frac{(p^2 + ap + \frac{q^2}{M^2})}{p + a} \tag{6.7}$$

$$s_u = \frac{M}{4}(p'_c - a) \tag{6.8}$$

p=p' Effective mean stress (compression is positive)

q Deviator stress

M Slope of the critical state line

p'_c Effective consolidation stress on the hydrostatic axis (=p_p in Figure 6.1)

s_u Undrained shear strength

The program PLAXIS calculated on this basis the value of the critical state parameter M=1,51.

Equations (6.7) and (6.8) do not include the initial values of the consolidation stress or the undrained shear strength before the subsoil was loaded. However, they can be calculated from Equations (6.9) to (6.11).

$$\sigma'_{yc} = \sigma'_{y0} + POP \tag{6.9}$$

$$p = p' = (2K_0^{NC} + 1)\frac{\sigma'_{yc}}{3} \tag{6.10}$$

$$q = (1 - K_0^{NC})\sigma'_{yc} \tag{6.11}$$

σ'_{y0} Effective vertical stress before construction

K_0^{NC} Coefficient of lateral earth pressure at rest

σ'_{yc} Effective vertical consolidation stress

POP A parameter that describes the overconsolidation conditions, see Equation (6.1)

The curves of Figure 6.6, Figure 6.7 and Figure 6.8 are obtained by substituting the calculated values of p' and q to Equations (6.7) and (6.8).

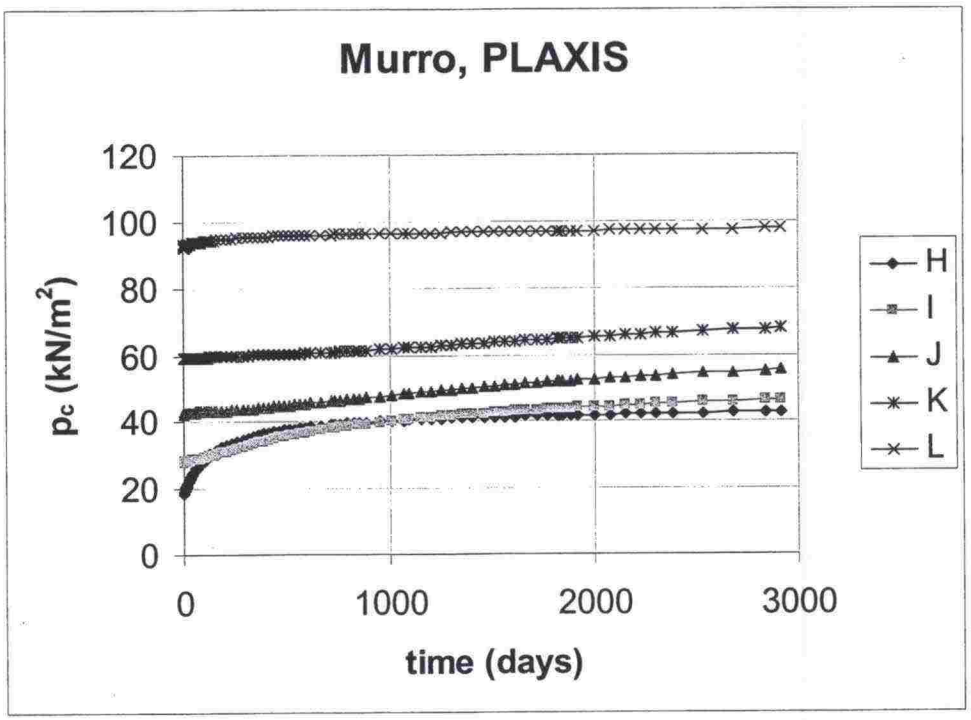

Figure 6.6 *The evolution of the effective consolidation stress in the points of interest during eight years.*

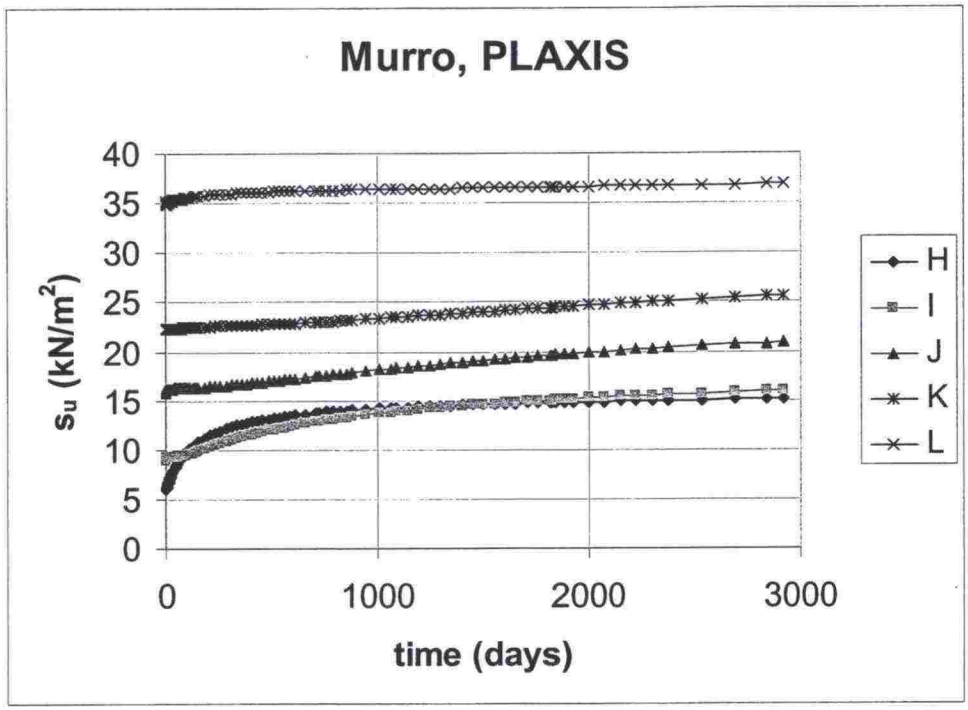

Figure 6.7 *The evolution of the undrained shear strength in the points of interest during eight years.*

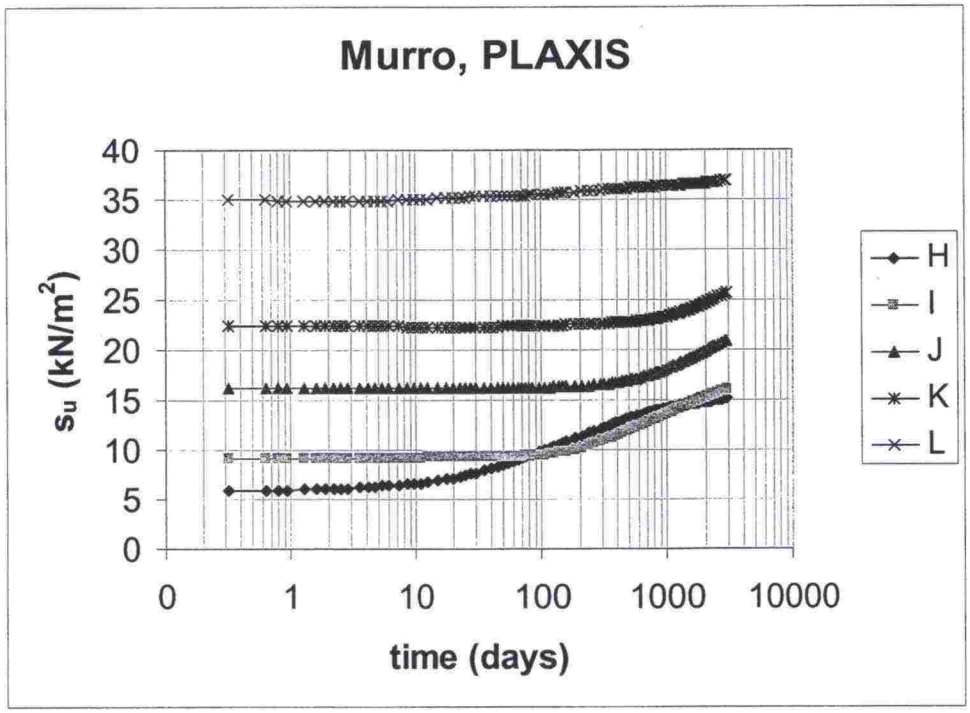

Figure 6.8 *The growth of undrained shear strength during eight years in logarithmic time scale.*

As a summary of the development of strength, the consolidation stresses and undrained shear strengths calculated with PLAXIS in the points of interest are presented in Table 6.6.

Table 6.6 Consolidation stresses and undrained shear strengths calculated with PLAXIS.

Point	p'_c , kPa before construction	p'_c , kPa 8 years after construction	s_u , kPa before construction	s_u , kPa 8 years after construction
H	18,84	43,07	6,11	15,26
I	27,75	47,68	8,97	16,50
J	42,16	56,70	15,91	21,40
K	59,26	69,57	22,37	26,26
L	93,19	100,20	35,18	37,82

On the basis of Table 6.6 some strengthening has happened in the soil. The process has mainly taken place in layers 2 and 3. The observations and laboratory tests support this fact. Figure 6.8 shows well the effect of consolidation process as for the development of undrained shear strength.

6.2 Calculations with SAGE CRISP

6.2.1 Initial data

The embankment material and the 1,6 meters thick heavily overconsolidated clay layer under the embankment was modelled in the SAGE CRISP-calculations with the original ideally elasto-plastic Mohr-Coulomb material model (MC model). The soft clay layers below that were modelled with the Modified Cam Clay model (MCC model). The yield surface of the MCC model in p'-q-plane is presented in Figure 6.9. The differences between the MCC model of SAGE CRISP and SS model of PLAXIS are:

- The yield surface of MCC model has no cohesion term
- The yield surface of MCC model is an ellipse in p'-q-plane from origin to preconsolidation pressure p'_c
- The yield surface of MCC model is a smooth ellipsoid without corners in three-dimensional principal stress space

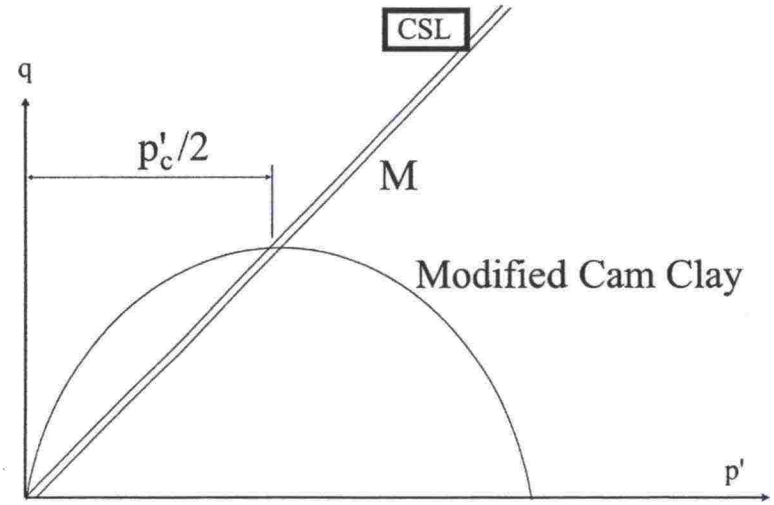

Figure 6.9 *The yield surface of MCC model in the co-ordinate system of mean effective stress p' and deviator stress q. M is the slope of the critical state line, p'_c is the effective consolidation stress on the hydrostatic axis.*

The layers and their parameters are presented in Tables 6.7...6.10.

Table 6.7 *The layers and overconsolidation conditions used in SAGE CRISP.*

Layer number	Soil type	Depth, m	Y co-ordinate	Material model
1a	Clay (OC)	0,0-1,0	23,0-22,0	MC
1b	Clay (OC)	1,0-1,6	22,0-21,4	MC
2	Clay (NC)	1,6-3,0	21,4-20,0	MCC
3	Clay (NC)	3,0-6,7	20,0-16,3	MCC
4	Clay (NC)	6,7-10,0	16,3-13,0	MCC
5	Clay (NC)	10,0-15,0	13,0-8,0	MCC
6	Clay (NC)	15,0-23,0	8,0-0,0	MCC
7	Embankment	-	-	MC

Table 6.8 *Parameters of the Modified Cam Clay –model, part 1.*

Layer number	γ kN/m^3	λ -	κ -	k_x m/year	k_y m/year
2	15,6	0,40	0,030	0,078	0,060
3	14,5	0,50	0,036	0,065	0,049
4	15,1	0,40	0,030	0,040	0,033
5	15,5	0,38	0,034	0,025	0,020
6	16,0	0,14	0,004	0,038	0,030

Table 6.9 Parameters of the Modified Cam Clay –model, part 2.

Layer number	ν -	e_{cs} -	c' kN/m^2	φ' °	M	K_0^{NC} -
2	0,35	2,77	0	37	1,0	0,7
3	0,10	3,92	0	37	1,0	0,7
4	0,15	3,39	0	37	1,0	0,7
5	0,15	3,16	0	37	1,0	0,7
6	0,15	2,15	0	37	1,0	0,7

Table 6.10 Parameters of the original Mohr-Coulomb model.

Layer number	γ kN/m^3	k_x m/year	k_y m/year	ν -	E MPa	c' kPa	φ' °
1a	16,2	-	-	0,35	11,3	2	39,2
1b	16,2	0,227	0,173	0,35	11,3	2	39,2
Embank-ment	19,6	-	-	0,35	40	2	40

Parameters presented in previous tables (SAGE CRISP technical reference manual 1999):

γ Total unit weight of soil

k_x Horizontal permeability

k_y Vertical permeability

ν Poisson ratio

E Young's modulus (MC)

c' Cohesion (=0 in MCC model)

φ' Friction angle (used only for calculation of M in MCC model)

M Slope of critical state line (MCC) (in plane strain state)

λ Slope of isotropic compression line, NC (MCC)

κ Slope of unload-reload lines, OC (MCC)

ε_{cs} Reference void ratio on critical state line when p' = 1 kPa

K_0^{NC} Coefficient of in situ earth pressure in normally consolidated state (for calculation of initial stresses)

The layers and the parameters are in principle the same as in the PLAXIS-calculations, except that the permeability has been decreased to one third of the original values. Because SAGE CRISP does not include a system for decreasing the permeability as the void ratio decrease, the value of perme-

ability had to be chosen according to the real stress state. Because cohesion is now zero, the critical state parameter is

$$M = \frac{6\sin\varphi}{3+\sin\varphi} \tag{6.12}$$

The reference void ratio e_{cs} on critical state line when p'=1 kPa can be calculated with Equations (6.13) ... (6.17):

$$e_{cs} = e_0 + (\lambda - \kappa)\ln p'_a - \kappa \ln p' \tag{6.13}$$

$$p'_a = p'_c / 2 \tag{6.14}$$

where e_0 is the initial void ratio (marked with e_{init} in Table 6.3). The effective consolidation stress p'_c:

$$p' = \sigma'_y (1 + K_0)/3 \tag{6.15}$$

$$q = (1 - K_0)\sigma'_y \tag{6.16}$$

$$p'_c = p' + \frac{(q/\mathrm{M})^2}{p'} \tag{6.17}$$

where σ_y' is the effective vertical stress in situ and $K_0 = K_0^{NC}$ for normally consolidated clays.

In SAGE CRISP, the consolidation stress is given as the effective preconsolidation pressure p'_c on the hydrostatic axis. In Figure 6.10 is presented its vertical distribution together with the effective vertical stress σ'_y, effective horizontal stress σ'_x and the pore pressure PVP.

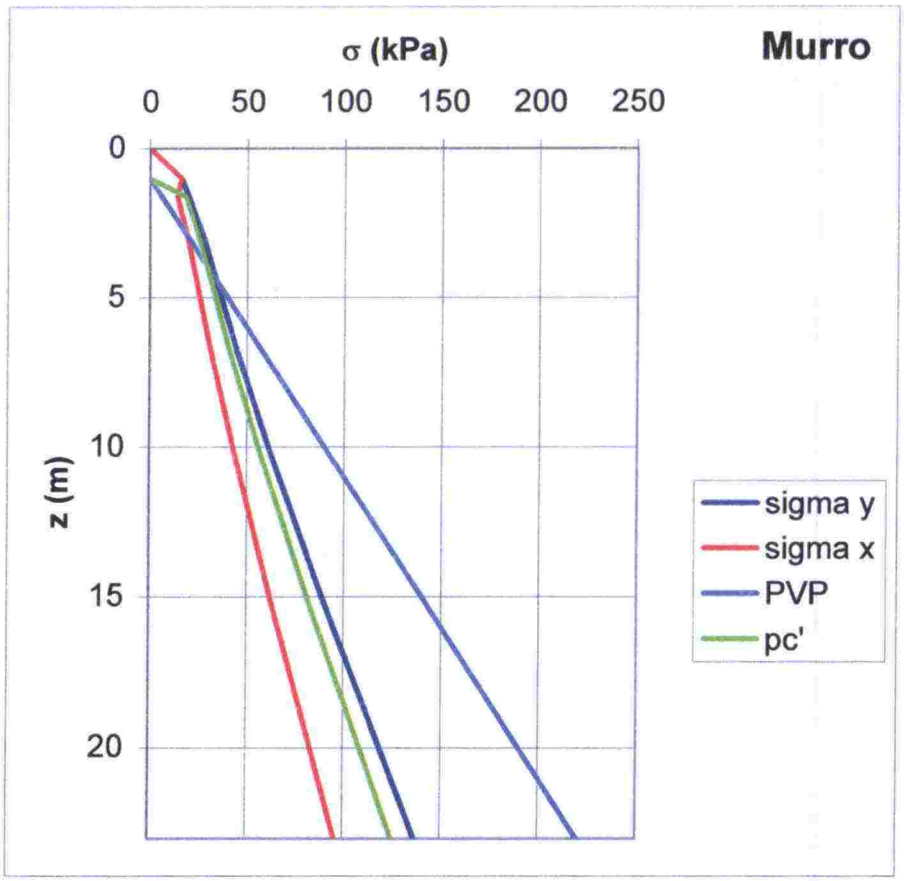

Figure 6.10 Distribution of the vertical in situ-stresses of Murro test embankment.

Rectangular 8-noded consolidation elements in plane strain conditions were used in calculations. The finite element mesh was built up using symmetry in the centre line of the embankment. The boundary conditions of consolidation were set to be valid already in the beginning of the construction stage. The boundary conditions were drained on the ground level and on the solid bed, but undrained on the symmetry axis and on the right hand side of the model.

The modelling order of the problem was the following.

1. Calculation of the initial stresses
2. Setting of the boundary conditions of consolidation
3. Adding the load in thin layers, beginning of the consolidation process
4. Calculation of the consolidation stage with small time increments

The incremental method specified by MDF-iteration was chosen for the non-linear solving method in the program SAGE CRISP. MDF stands for Modified Newton-Raphson –iteration, which is also called the initial stress iteration (Vepsäläinen 1983). The MDF-iteration requires significantly longer calculation time but reduces the methodological and calculation errors that disrupt the stress equilibrium conditions.

6.2.2 Results of the calculations

In this section the settlements, pore pressures and horizontal displacements calculated with the program SAGE CRISP are studied. In addition, evolution of stress paths and the void ratio are studied in the subsoil under the centre line of the embankment during the consolidation process.

The calculated and observed settlements are shown in Figure 6.11 and in Figure 6.12 in linear and logarithmic time scale.

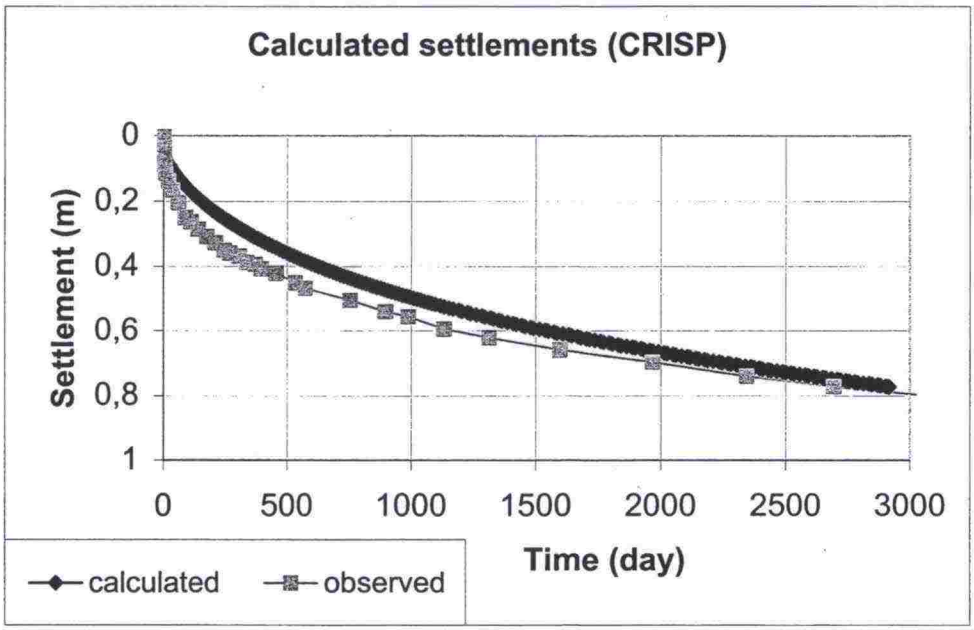

Figure 6.11 *The settlement of the ground surface under the centre line of Murro test embankment in linear time scale. The observed and the calculated values are compared.*

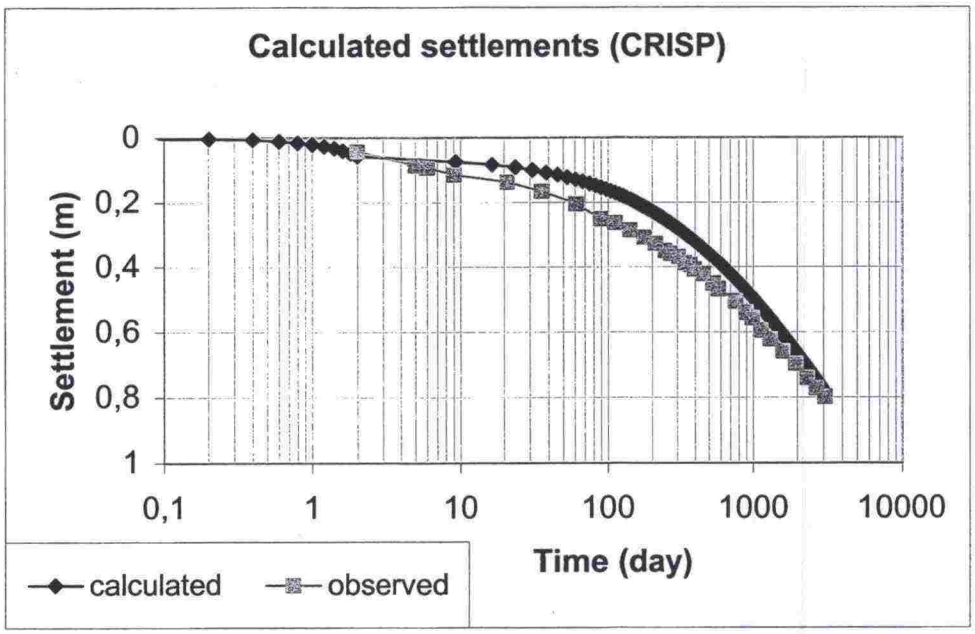

Figure 6.12 *The settlement of the ground surface under the centre line of Murro test embankment in logarithmic time scale. The observed and the calculated values are compared.*

On the basis of Figure 6.12 can be said that the calculated settlements correspond well to the observed ones as for eight years time. During the first year, the calculated curve falls behind the observed settlements, but the curves start to balance out after that.

Figure 6.13 presents the calculated settlements under the embankment on the boundaries of the layers. The points of interest correspond to the points chosen for PLAXIS-calculations (see Figure 6.3). Figure 6.13 shows that the calculated settlements are distributed to a little thicker layer than observed.

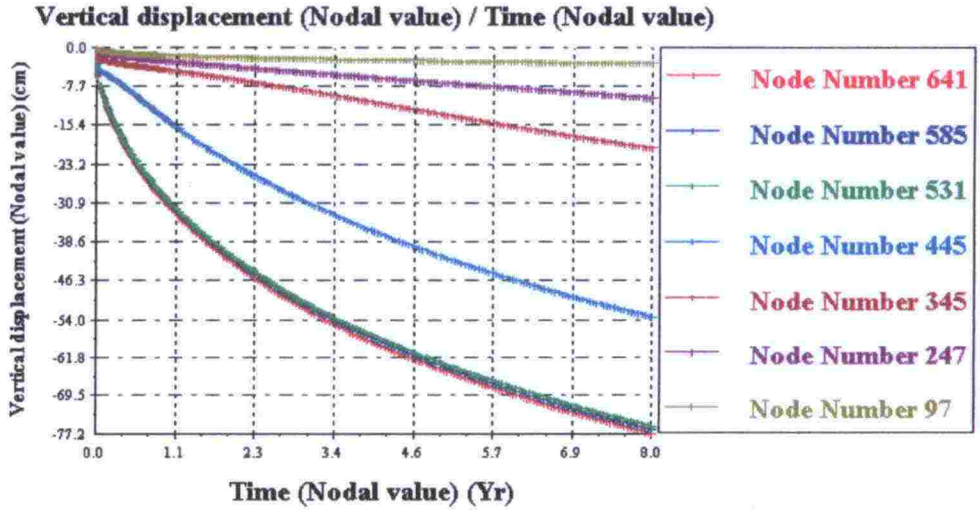

Figure 6.13 Calculated settlements (SAGE CRISP) by layer under the centre line of Murro test embankment.

The settlement of the ground surface is shown in Figure 6.14. The edge of the top of the embankment is at x-coordinate of 500 cm and the toe at x-coordinate of 900 cm. It can be seen that the ground surface settles slightly right next to the embankment as well. The increment numbers correspond to following times:

- Inc no 11 - right after the construction of the embankment
- Inc no 61 - 1 year from the beginning of the construction
- Inc no 111 - 3 years from the beginning of the construction
- Inc no 211 - 8 years from the beginning of the construction

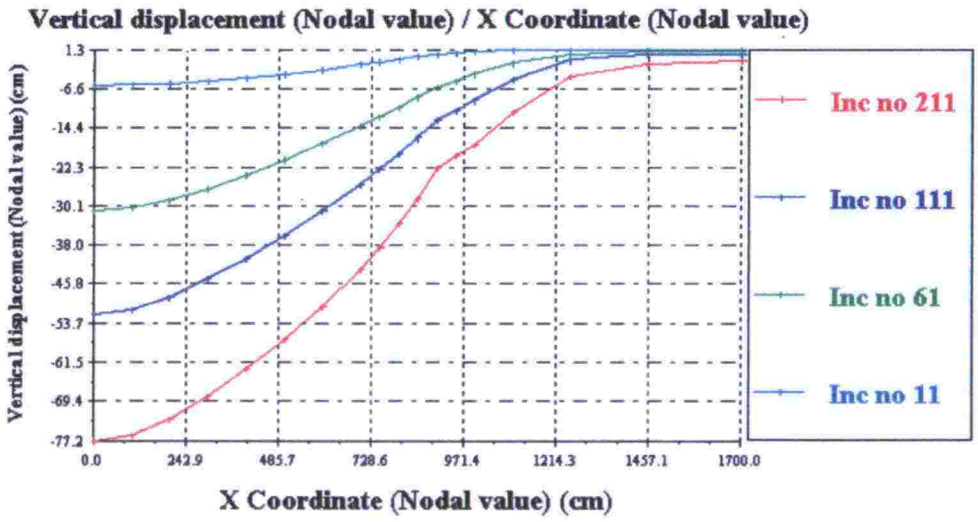

Figure 6.14 The settlement of the ground surface under Murro test embankment.

Figure 6.15 shows the calculated horizontal displacements underneath the toe of the embankment. Compared to the observed values, the magnitude is again predicted well, but the depth of the maximum is slightly smaller than observed.

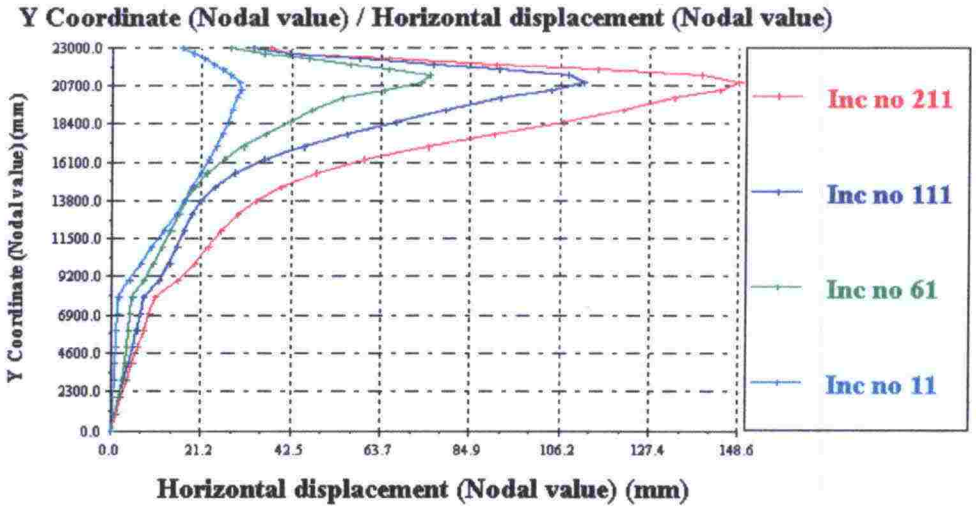

Figure 6.15 The calculated horizontal displacements on the bottom of the slope of Murro test embankment.

The development of the total pore pressures until eight years of construction is presented in Figure 6.16 by integration points. Their positions in the sub-soil below the centre line of the embankment are presented in Table 6.11. The initial pore pressures by layers (PVP) can be found in Figure 6.10 and are presented in Table 6.11, too.

Table 6.11 The positions of the integration points in the subsoil under the centre line of Murro test embankment.

IP Number	Layer	Depth, m	PVP, kPa	Corresponding point in PLAXIS-calculations (see Table 6.5)
5044	2	2,1	11	H
4454	3	4,1	31	I
3019	4	7,7	67	J
2267	5	11,5	105	K
944	6	18,5	175	L

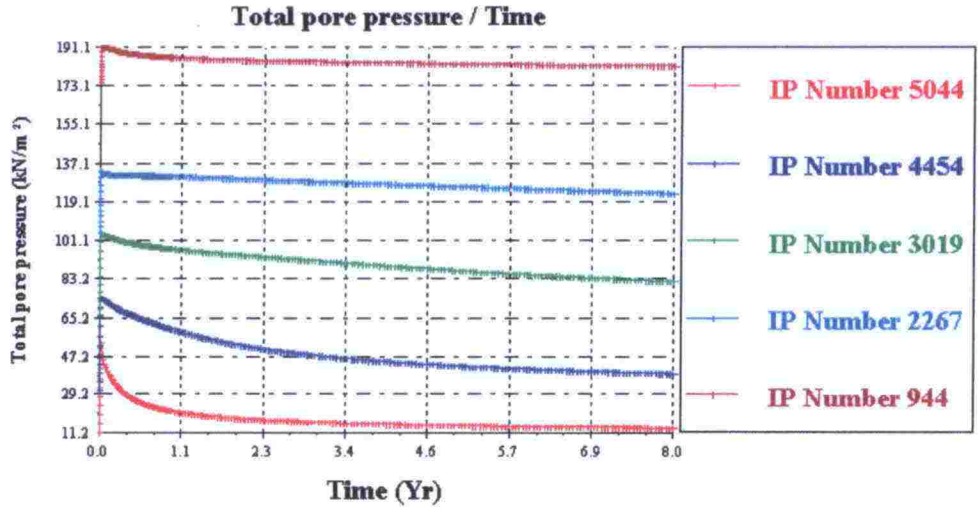

Figure 6.16 The calculated development of the total pore pressures during eight years from construction.

Figure 6.17 presents the calculated distribution of the excess pore pressures under the centre line of Murro test embankment. The noise in the curve of increment number 11 (right after the construction of the embankment) is due to numerical errors when changing from real values in integrating points to approximate nodal values in the beginning of the consolidation process.

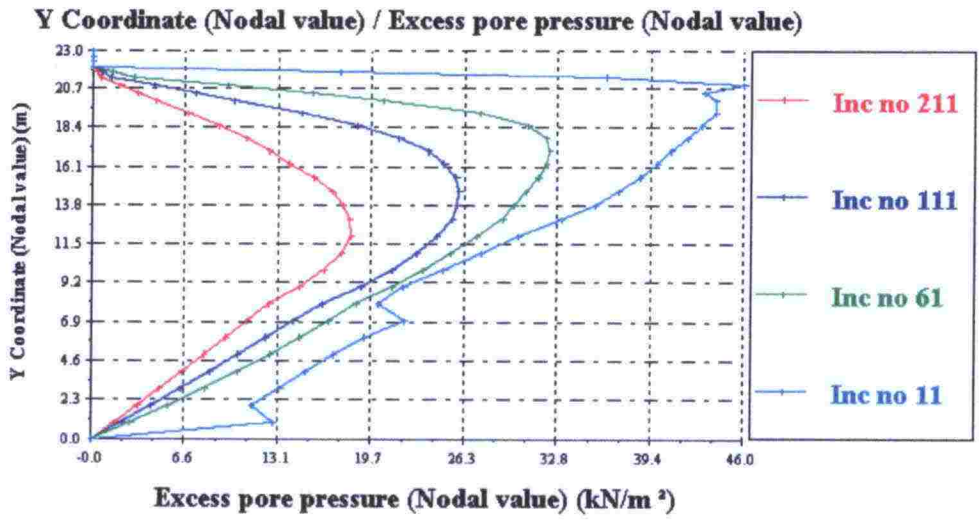

Figure 6.17 The calculated distribution of the excess pore pressures under the centre line of Murro test embankment.

The conversion of the void ratio in the integration points is shown in Figure 6.18. The deepest points show very little decrease in the void ratio whereas in the two upper points the void ratio decreases with 0,25 (point 4454) and 0,35 (point 5044).

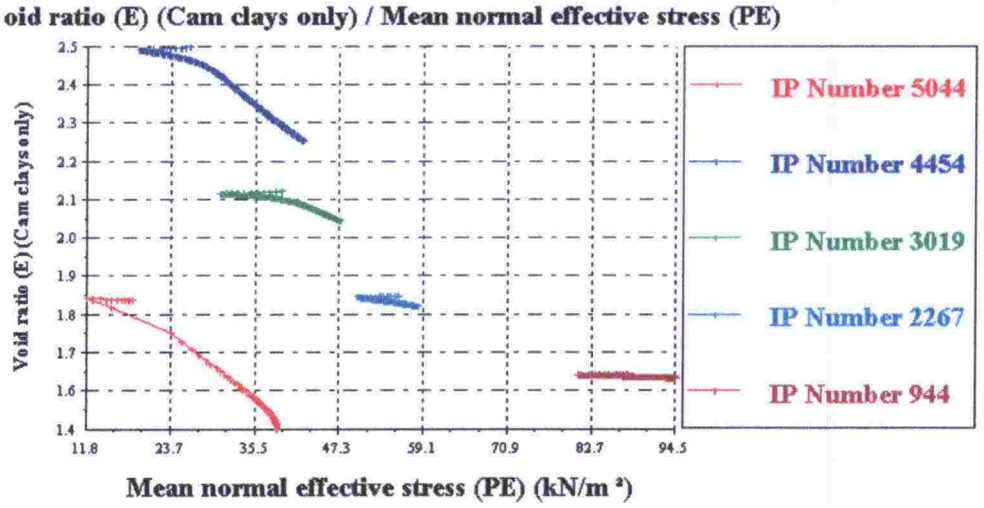

Figure 6.18 The conversion of the void ratio during eight years.

Figure 6.19 and Figure 6.20 present the stress paths in q-p' plane and u-p' plane, respectively.

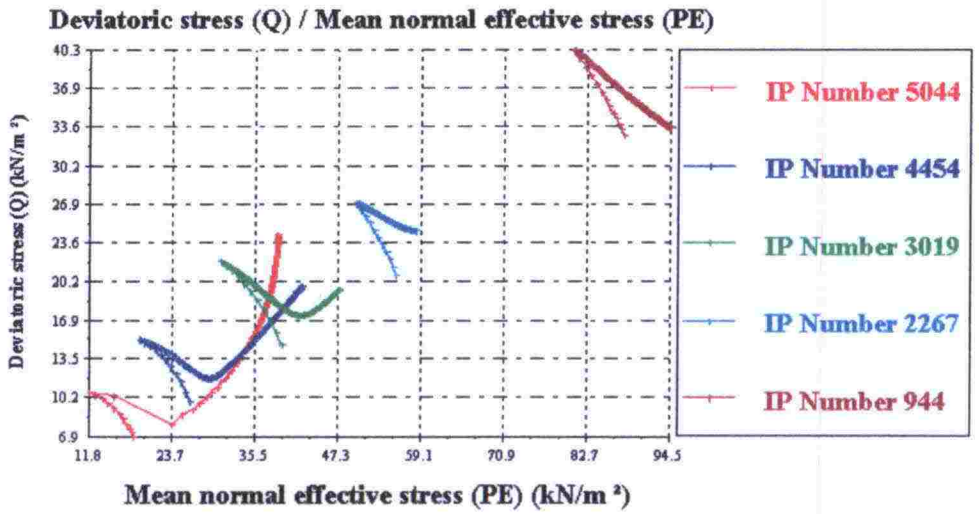

Figure 6.19 The stress paths q-p' in the points of interest.

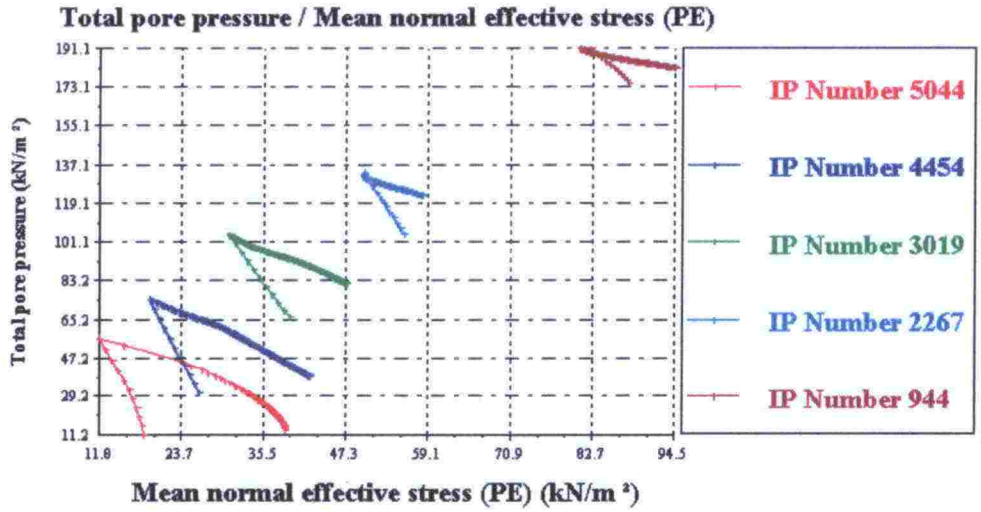

Figure 6.20 Stress paths u-p' in the points of interest.

The stress paths in q-p' plane and the corresponding yield surfaces are presented in Figure 6.21 to Figure 6.25.

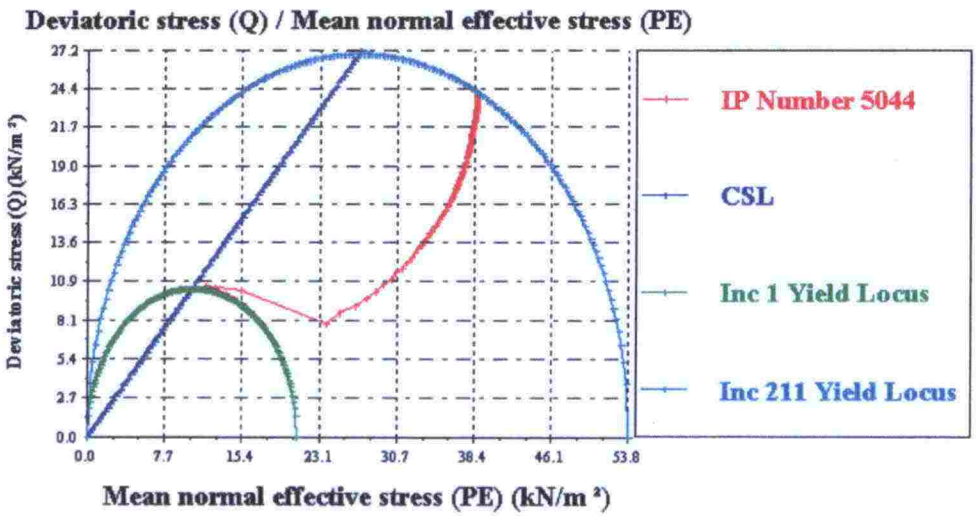

Figure 6.21 The stress path of IP 5044 (point H), 2,1 meters below ground surface.

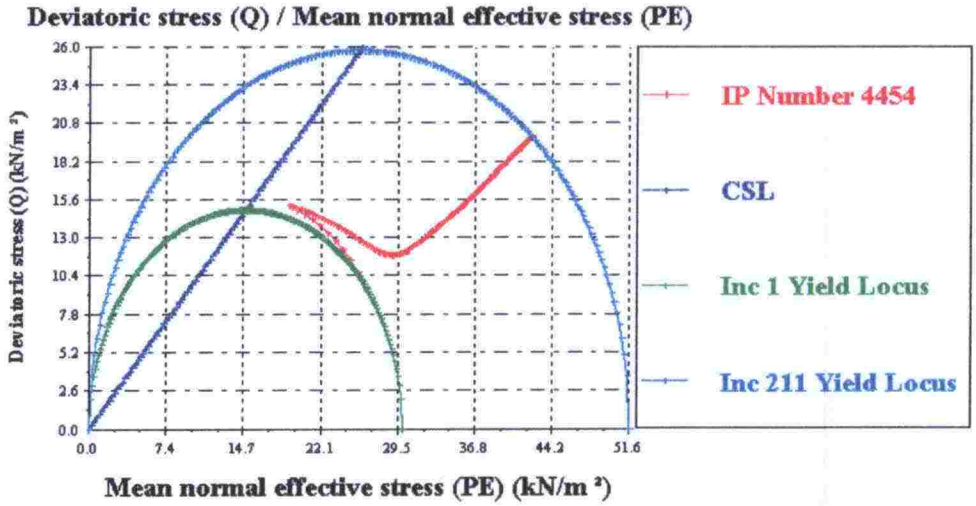

Figure 6.22 The stress path of IP 4454 (point I), 4,1 meters below ground surface.

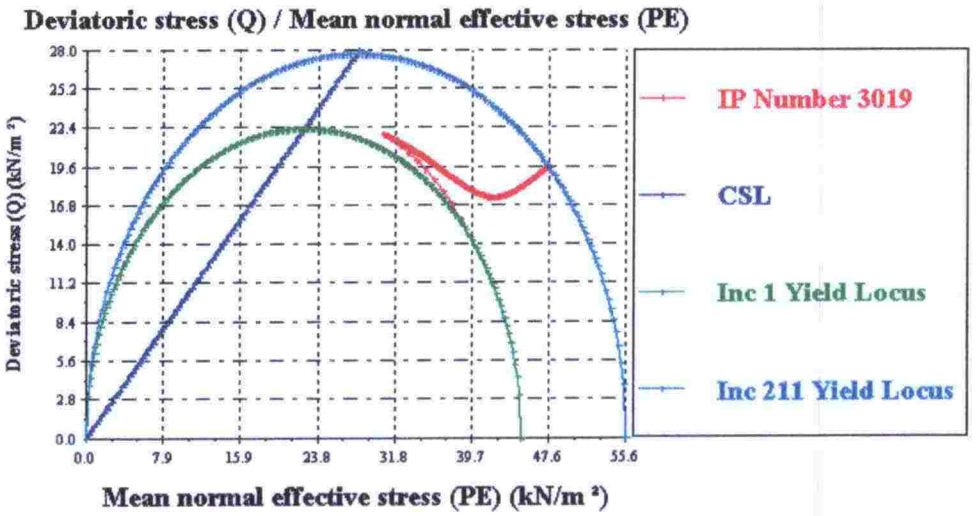

Figure 6.23 The stress path of IP 3019 (point J), 7,7 meters below ground surface.

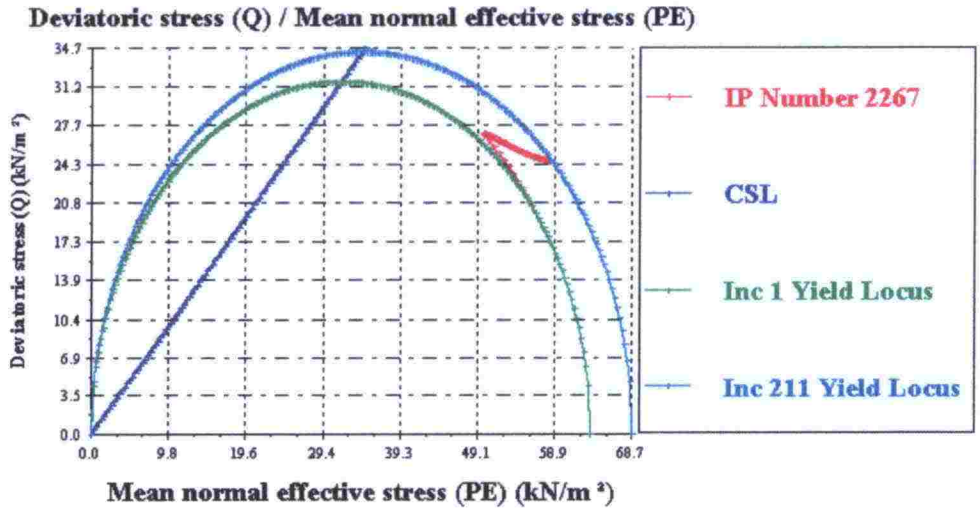

Figure 6.24 The stress path of IP 2267 (point K), 11,5 meters below ground surface.

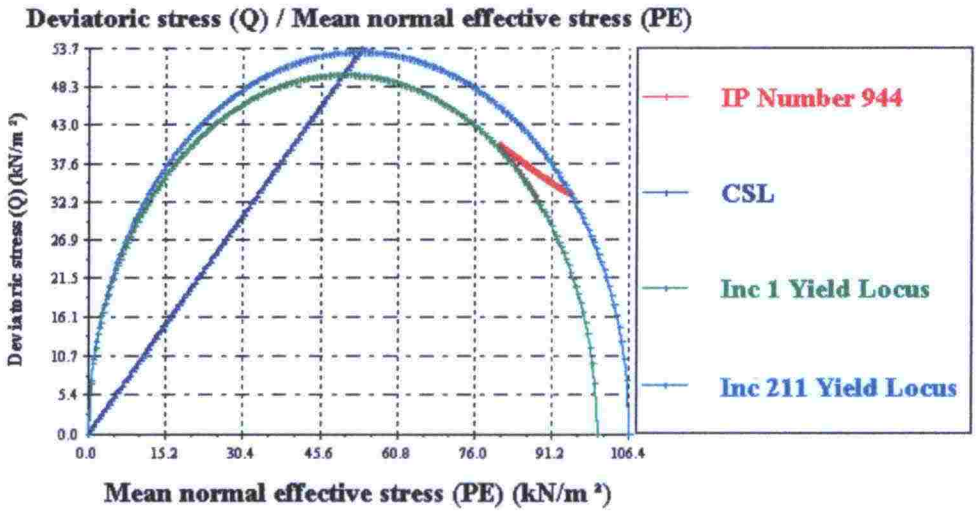

Figure 6.25 The stress path of IP 944 (point L), 18,5 meters below ground surface.

The growth of the undrained shear strength during eight years is presented in Table 6.12. The maximum growth that is 8,3 kPa happens in the uppermost soft layer. In the layer below that the growth is still 5,4 kPa, but in the other layers less than 3 kPa. Compared to results calculated with PLAXIS, these are of the same magnitude.

Table 6.12 The growth of the shear strength of Murro clay during eight years calculated with SAGE CRISP.

Point	Depth, m	s_u, kPa before construction	s_u, kPa after 8 years
5044	2,1	5,2	13,5
4454	4,1	7,5	12,9
3019	7,7	11,3	13,9
2267	11,5	15,9	17,2
944	18,5	25,0	26,6

7 CONCLUSIONS

Murro test embankment was constructed in Seinäjoki in 1993 by the Finnish Road Administration. The deposit in Murro is 23 meters thick and consists of normally consolidated clayey silt and silty clay. It can be roughly divided into two layers with similar thickness. The shear strength of the upper layer is between 10 kPa and 20 kPa, and the shear strength of the lower layer is about 30 kPa. In pursuance of construction, the embankment was instrumented: settlement plates, extensometers, inclinometers and pore pressure probes were installed, and the data has been collected for eight years. In 2001, eight years after construction, a comprehensive sounding and laboratory testing program was carried out both under and next to the embankment.

The first object of the project was to study the strengthening of the subsoil and the behaviour of the embankment. The information of the test embankment was meant to be used for the design of a road embankment nearby on the same deposit as well as for design and improvement of other roads built on soft soils. That is a part of a long-term project TPPT Road Structures Research Program.

The second object is to study, if this embankment is a suitable subject for developing and testing a new soil model. The latter object is a focus of a European Research Training Network, Soft Clay Modelling for Engineering Practice, alias SCMEP. The Finnish Academy has, partly in context with SCMEP, funded two projects: Modelling of mechanical behaviour of naturally anisotropic soft soils (1998-2000) and De-structuration of natural soft clays. The latter begun on 1st January 2002 at Helsinki University of Technology and it continues for three years. Murro test embankment is thought to be a convenient research subject for the new Finnish Academy project due to the very comprehensive observations of behaviour of soft soil over a relatively long period. The triaxial test series presented in Section 5.4 supports this intention, and another test series on reconstituted Murro clay is going to be carried out soon.

In order to study the increase in undrained shear strength, calculations with programs PLAXIS and SAGE CRISP were carried out and compared to the observations. For the dry crust, Mohr-Coulomb model was used in both programs. In the PLAXIS calculations, the Soft Soil –model without creep was used for modelling the soft soil layers. Considering the effect of creep was thought to be unnecessary because of relatively high pore pressures still after eight years. The outcome of the calculations was fairly successful. The calculated eight-year settlement was 76,7 cm as the observed settlement was 79,8 cm. The horizontal displacements were 10,6 cm and 12,3 cm, respectively. The depth of the maximum displacements differed slightly, though. The parameters used in the calculations were checked on the basis

of the settlements, and no need for updating them was observed. The calculated growth of the shear strength was up to 9 kPa in the softest layers. Comparison with the observed values is difficult because the reliability of the field vane test results is a little questionable in this case, and the fall cone test results show no increase in undrained shear strength. On the basis of the penetration tests it is difficult to see any dramatic changes either.

In SAGE CRISP, Modified Cam Clay was chosen for modelling the soft soil layers. The parameters were chosen to be the same as in PLAXIS-calculations except the values of permeability that were taken as one third of those used in PLAXIS. The results of the calculations were again rather successful. The calculated settlement was 77,2 cm and the horizontal displacement 14,6 cm. Both values correspond well to the observed values. Comparison between Figure 4.8 and Figure 6.18 shows that the calculated decrease of the void ratio corresponds to the observed one. The void ratio has decreased in the softest layers only, and it should explain the settlements that have happened in the soil below the centre line of the embankment. The calculated growth of the undrained shear strength can again be noticed in the two softest layers. The maximum growth is about 8 kPa.

It should be noticed, that the value of the critical state parameter M cannot be used directly from the triaxial tests in neither of the programs but should be modified to the plane strain state. More calculations about Murro test embankment have been published by Länsivaara (2001). Those calculations evaluate different methods for predicting further settlements with the help of current observations, for instance the settlement potential method, Asaoka method and the hyperbola method.

As mentioned, Murro test embankment is a good object for studies because of the quantity of good observations, site investigations and laboratory tests. The calculations were successful and show that further investigations of Murro embankment are viable.

REFERENCES

Brinkgreve, R.B.J., Vermeer, P.A. (editors). PLAXIS Finite Element Code for Soil and Rock Analyses, Version 7. A.A. Balkema, Rotterdam, Brookfield, 1998.

Dafalias, Y.F., 1987. Anisotropic critical state clay plasticity model. Proc. of 2nd Int. Conf. on Constitutive Laws for Engineering Materials, Tucson, Arizona, Vol. I. Elsevier, p. 513-521.

Janbu, N., 1970. Grunnlag in geoteknik. Trondheim, 426 p.

Korhonen, K-H., Lojander, M., 1987. Yielding of Perno clay. Proc. of 2nd Int. Conf. on Constitutive Laws for Engineering Materials, Tucson, Arizona, Vol. I. Elsevier, p. 1249-1255.

Koskinen, M., 2001. Anisotropy and de-structuration of soft clays. Master's Thesis, Helsinki University of Technology, 81 p.

Koskinen, M., 2001. Anisotropy and de-structuration of POKO clay. SCMEP, Workshop 2, 16-19 September, Graz, Austria, 24 p.

Länsivaara, T., 2001. Settlement predictions based on observational approach (in Finnish). Finnish National Road Administration, Finnra Reports 49/2001. 87 p. + app. 289 p.

Näätänen, A., Lojander, M., Wheeler, S., Karstunen, M., 1999. Experimental investigation of an anisotropic hardening model for soft clays. Proc. of the 2nd International Symposium on Pre-Failure Deformation Characteristics of Geomaterials, Torino, Italy, 28-30 September. Rotterdam, A.A. Balkema, p. 541-548.

Roscoe, K.H., Burland, J.B., 1968. On the generalised stress-strain behaviour of 'wet' clay. Engineering plasticity, Cambridge University Press, p. 553-569.

Selkämaa, E., 1994. Test embankment Seinäjoki, Murro (in Finnish). Graduate project, Seinäjoen teknillinen oppilaitos, Rakennustekniikan osasto, 27 p.

Vepsäläinen, P., 1983. The analysis of settlement, bearing capacity and stability by the Finite Element Method (in Finnish). Licentiate's Thesis, Helsinki University of Technology.

Wheeler, S.J., Näätänen, A., Karstunen, M., 1999. Anisotropic hardening model for normally consolidated soft clay. Proc. of 7th International Sympo-

sium on Numerical Models in Geomechanics (NUMOG), Graz, Austria. Rotterdam, A.A. Balkema, p. 33-44.

Wheeler, S., 2001. Destructuration – where are we now? SCMEP, Workshop 2, 16-19 September, Graz, Austria, 23 p.

Wood, D.M., 1990. Soil behaviour and critical state soil mechanics. Cambridge University Press, Cambridge.

Woods, R., Rahim, A., 1999. SAGE CRISP technical reference manual. For use with SAGE-CRISP version 4. SAGE Engineering Ltd.

APPENDICES

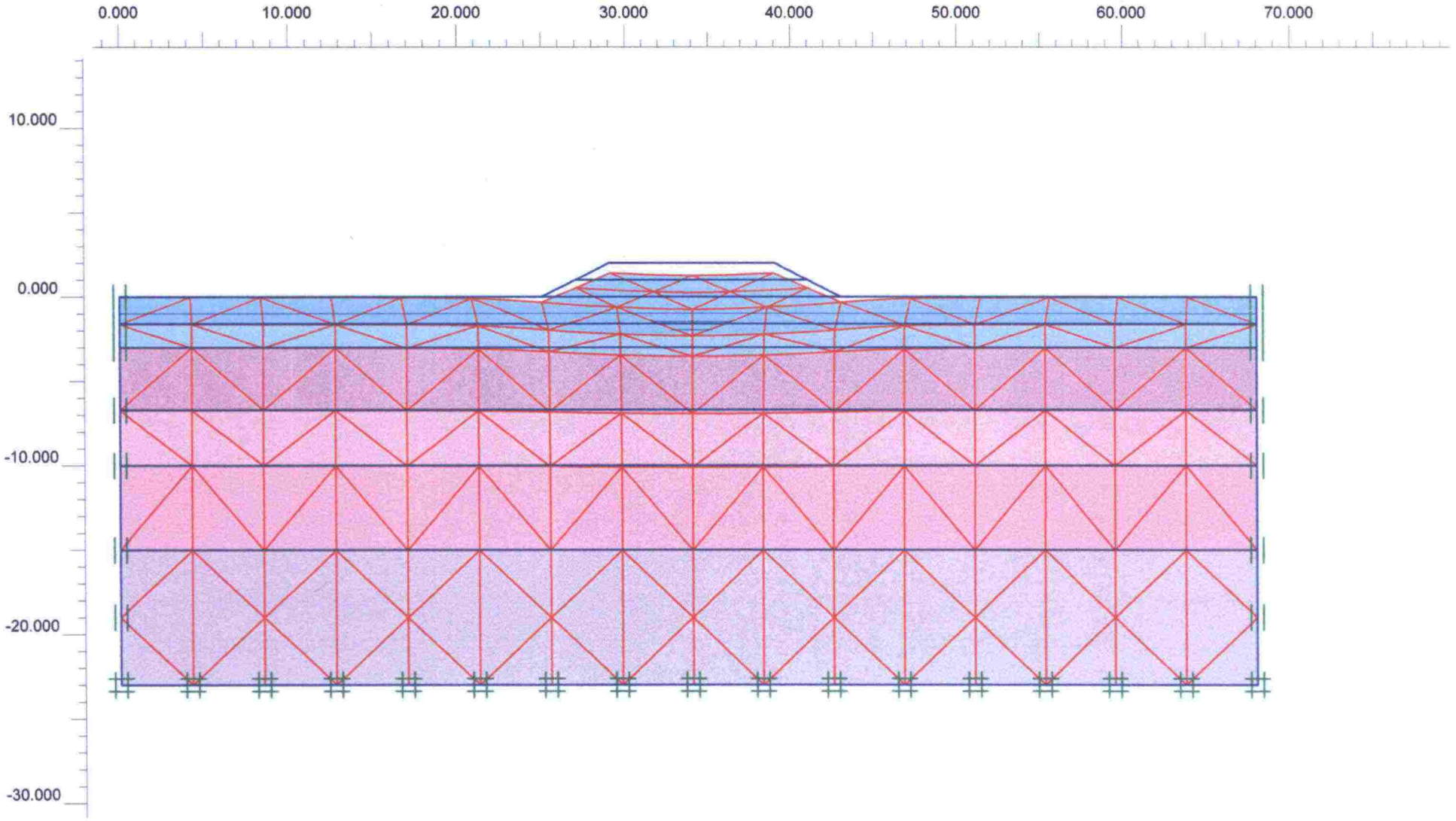

Deformed Mesh
Extreme total displacement 758,19*10^{-3} m
(displacements at true scale)

PLAXIS
Finite Element Code for Soil and Rock Analyses
Version 7.2.9.147

Project description
Appendix 1. Deformed element mesh 8 years after construction

Project name	*Step*	*Date*	*User name*
murro-5	108	16.04.02	Helsinki University of Technology

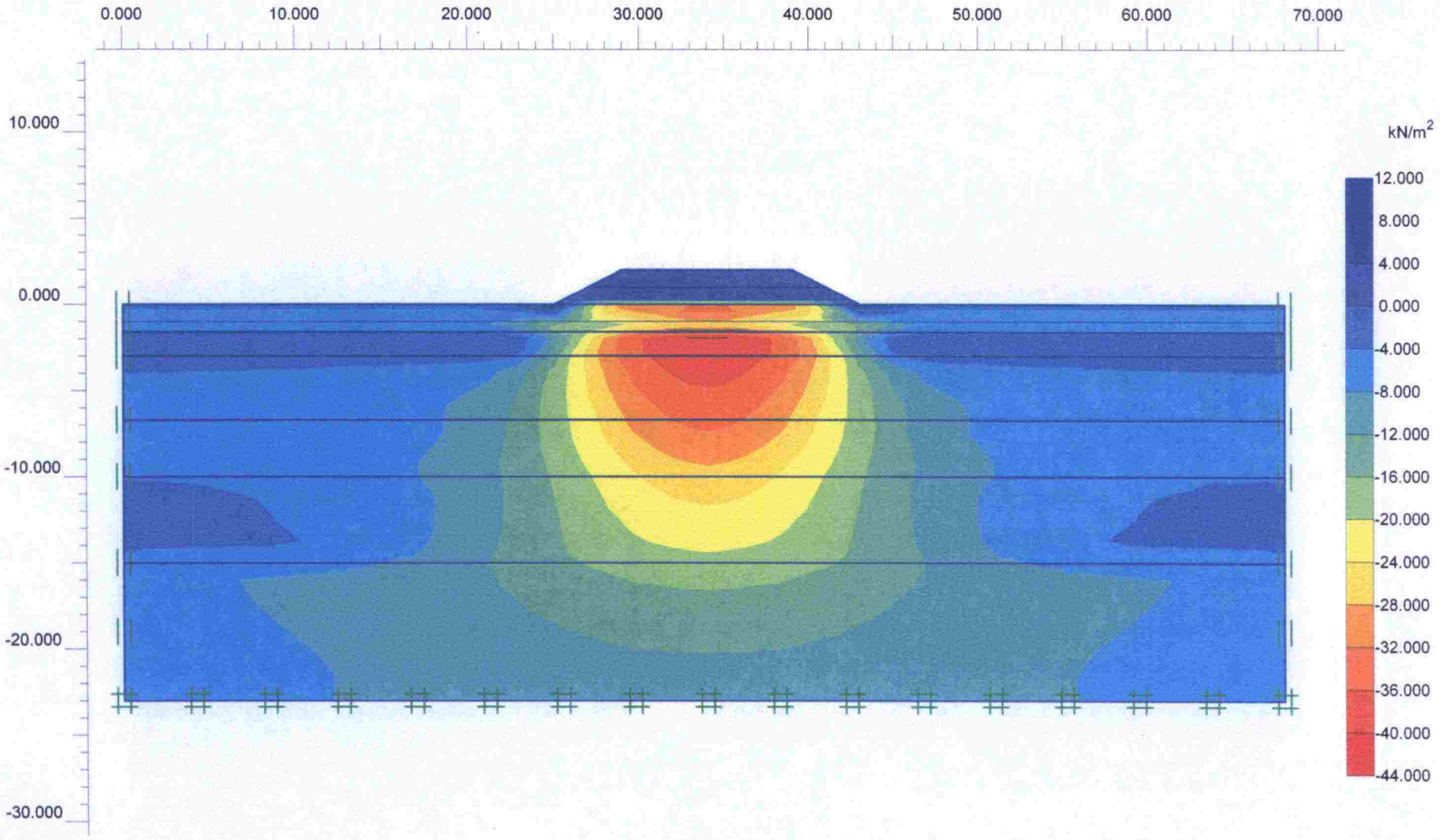

Excess pore pressures
Extreme excess pore pressure -40,13 kN/m^2
(pressure = negative)

PLAXIS
Finite Element Code for Soil and Rock Analyses
Version 7.2.9.147

Project description
Appendix 2a. Excess pore pressure immediately after construction

Project name	*Step*	*Date*	*User name*
murro-5	5	16.04.02	Helsinki University of Technology

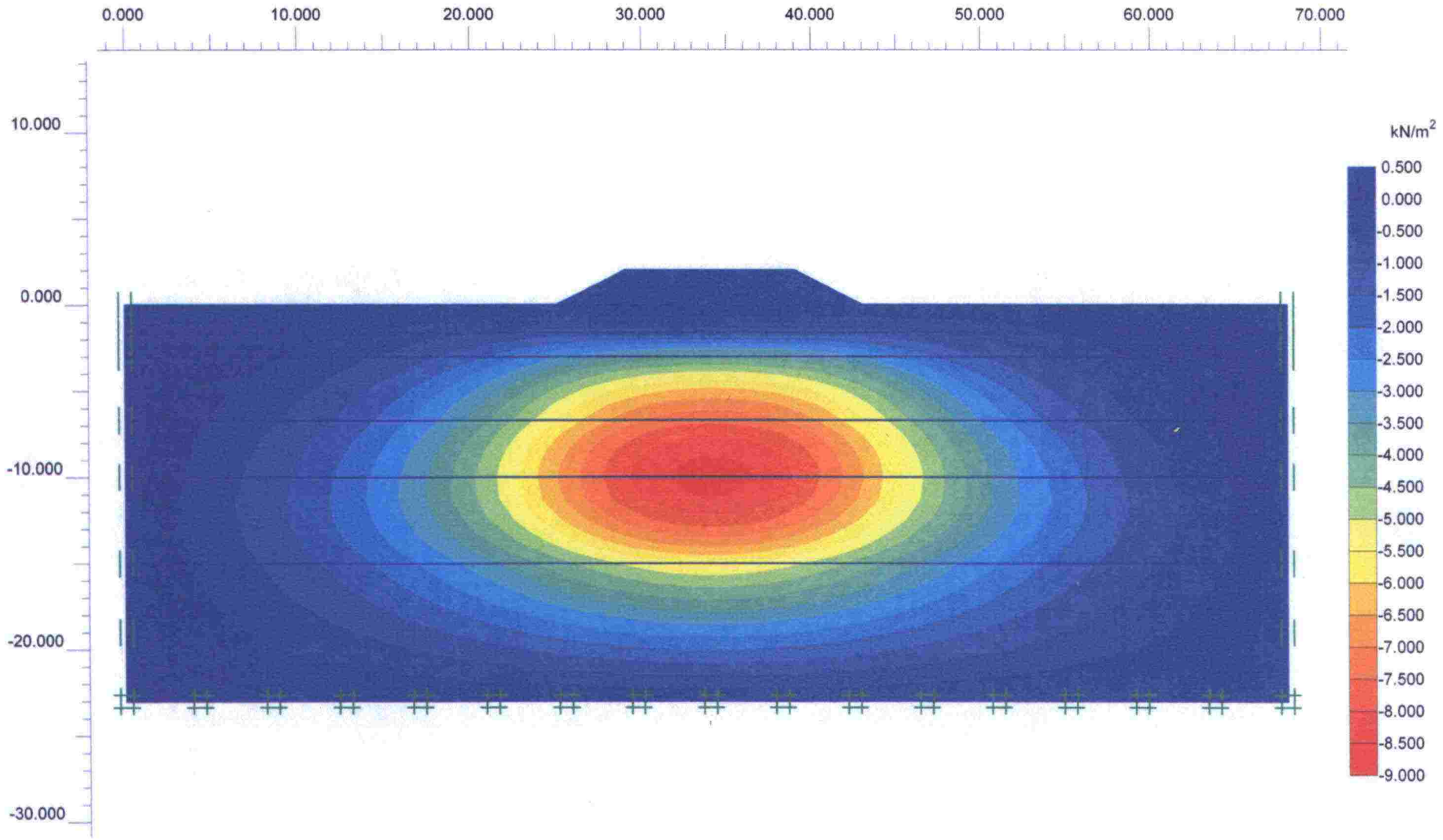

Excess pore pressures
Extreme excess pore pressure -8,69 kN/m^2
(pressure = negative)

PLAXIS
Finite Element Code for Soil and Rock Analyses

Project description
Appendix 2b. Excess pore pressure 8 years after construction

Project name	*Step*	*Date*	*User name*
murro-5	108	16.04.02	Helsinki University of Technology

Version 7.2.9.147

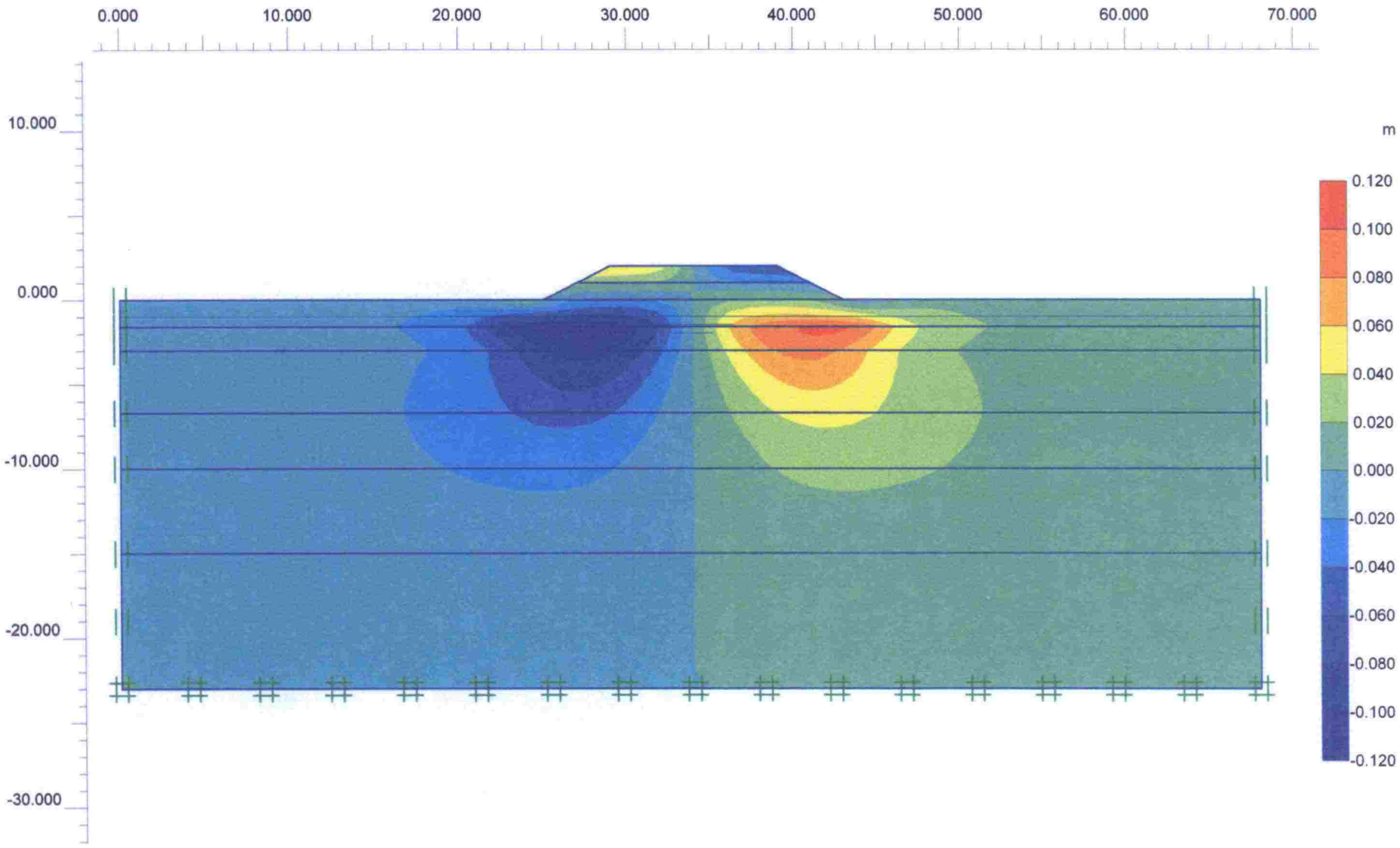

Horizontal displacements
Extreme horizontal displacement $106{,}07*10^{-3}$ m

PLAXIS
Finite Element Code for Soil and Rock Analyses
Version 7.2.9.147

Project description
Appendix 3. Horizontal displacements 8 years after construction

Project name	*Step*	*Date*	*User name*
murro-5	108	16.04.02	Helsinki University of Technology

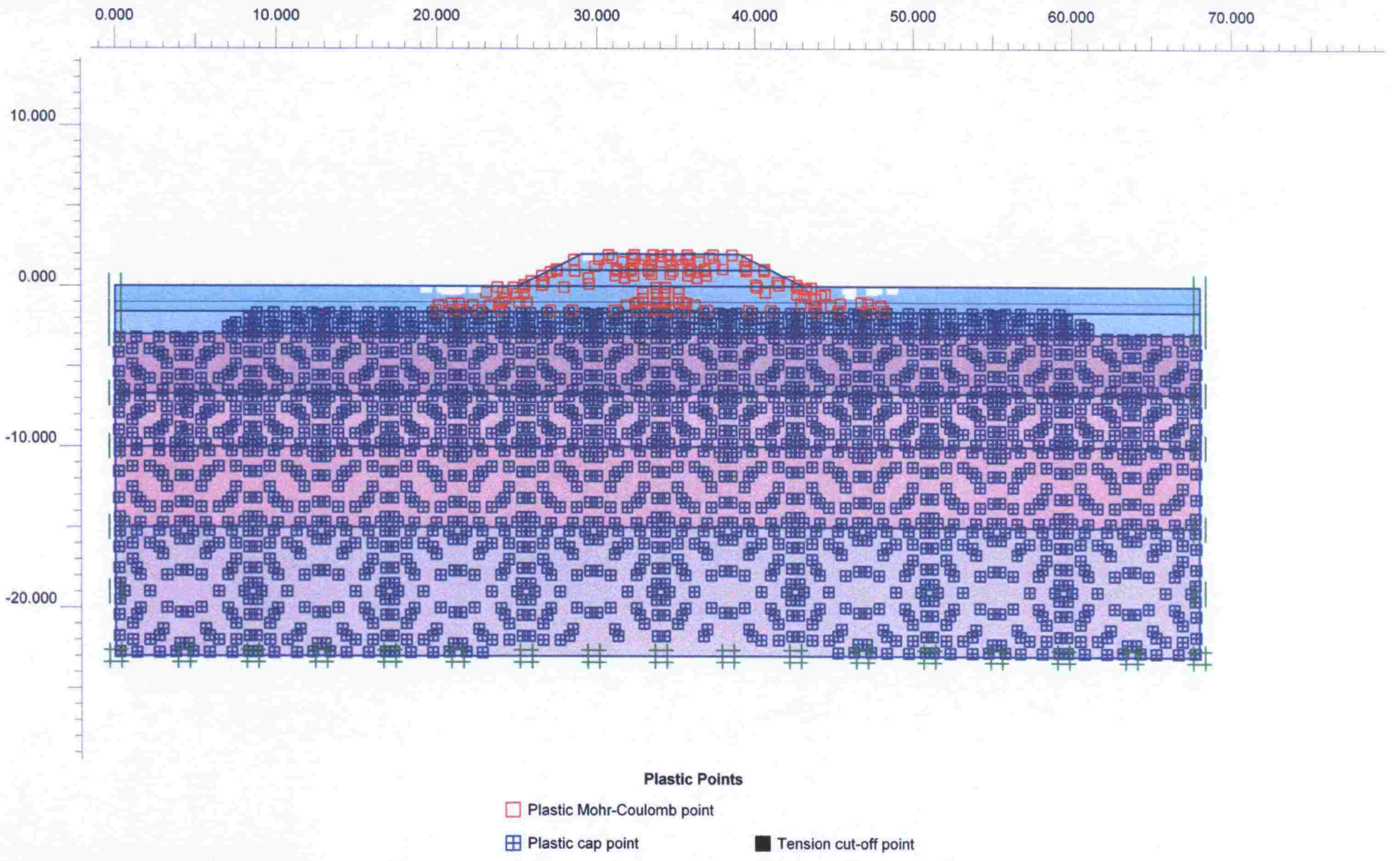

PLAXIS
Finite Element Code for Soil and Rock Analyses
Version 7.2.9.147

Project description

Appendix 4. Plastic points 8 years after construction

Project name	*Step*	*Date*	*User name*
murro-5	108	16.04.02	Helsinki University of Technology

ISSN 1457-9871
ISBN 951-726-883-1
TIEH 3200748E